Progressive Damage Analysis of Open Cut-out CFRP Laminates under Transverse Bending

Kalariya Yagnik Pravinchandra

A Thesis Submitted to

Indian Institute of Technology Hyderabad

In Partial Fulfillment of the Requirements for

The Degree of Master of Technology

भारतीय प्रौद्योगिकी संस्थान हैदराबाद
Indian Institute of Technology Hyderabad

Department of Mechanical and Aerospace Engineering

June 2015

Declaration

I declare that this written submission represents my ideas in my own words, and where ideas or words of others have been included, I have adequately cited and referenced the original sources. I also declare that I have adhered to all principles of academic honesty and integrity and have not misrepresented or fabricated or falsified any idea/data/fact/source in my submission. I understand that any violation of the above will be a cause for disciplinary action by the Institute and can also evoke penal action from the sources that have thus not been properly cited, or from whom proper permission has not been taken when needed.

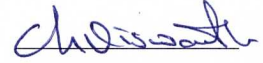(Signature)

Kalariya Yagnik Pravinchandra
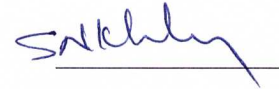
(Kalariya Yagnik Pravinchandra)
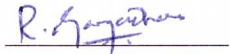
ME13M1009

(Roll No.)

Approval Sheet

This Thesis entitled Progressive Damage Analysis of Open Cut-out CFRP Laminates under Transverse Bending by Kalariya Yagnik Pravinchandra is approved for the degree of Master of Technology from IIT Hyderabad

(Dr. Viswanath Chinthapenta, Asst. Professor) Examiner
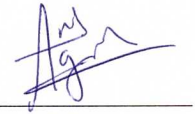Dept. of Mechanical and Aerospace Engineering
IITH

(Dr. Syed Nizamuddin Khaderi, Asst. Professor) Examiner
Dept. of Mechanical and Aerospace Engineering
IITH

(Dr. Gangadharan Raju, Asst. Professor) Examiner
Dept. of Mechanical and Aerospace Engineering
IITH

(Dr. M Ramji, Asso. Professor) Adviser
Dept. of Mechanical and Aerospace Engineering
IITH

(Dr. Anil Agarwal, Asst. Professor) Chairman
Dept. of Civil Eng
IITH

Acknowledgements

Dedication

Dedicated to my beloved parents

Abstract

In the present study, progressive failure analysis of carbon fiber reinforced polymer (CFRP) panel is carried out under flexural loading. The flexural properties of CFRP panels are characterized using four-point bend fixture and the same fixture is used to perform failure analysis of CFRP panels have different open cut-outs in form of multiple holes. The interaction between multiple holes with different configuration like two holes in longitudinal direction (2HL), transverse direction (2HT) or in diagonal direction (2HD) are carefully studied. Experiments are carried out using digital image correlation (DIC) to measure through-the-thickness strain distribution in all configurations. Failure propagation, final failure load and load-displacement profiles are analysed and compared with each other. Later, a finite element based progressive damage modelling (PDM) is implemented to study the damage initiation and propagation in CFRP panels. The predicted load-displacement profiles through PDM are compared with experimental results. Initially Hashin's criteria is used to predict intra-laminar failures with Ye's failure criteria for delamination. Afterwards, an advanced LaRC04 failure criteria is implemented for better prediction. Also delamination is introduced through cohesive zone modelling(CZM). LaRC04 failure criteria is based on fracture mechanism which needs to find out energy release rates (ERR) in mode I and mode II for CFRP panels. They are also required for implementing CZM. Double cantilever beam (DCB) test and end notch flexural (ENF) test are performed to extract mode I and mode II ERRs.

DIC system is used to find fracture toughness without measuring delamination length in case of DCB test. CZM properties are successfully calibrated to the experimental results. Viscous regularization in CZM is used to avoid the convergence issues. In the end, the comparison between different progressive damage models and experimental results are carried out. CFRP panels with 2HL configuration is found to have high load carrying capacity. Both failure theories failed to predict the final failure.

Contents

List of Figures

List of Tables

Chapter 1

Introduction and literature review

1.1 Introduction

Composites have made their presence across many applications, products and industries due to the distinct advantages over conventional materials. A composite is a material system that is made by combining two or more constituents or components on macro scale to get the best combination of properties which cannot be achieved using any of the constituents alone. In fiber reinforced composites, fiber has high strength and modulus acting as a discontinuous phase embedded in matrix acting as a continuous phase holding fibers together and transferring load between them.

Carbon fiber reinforced polymer (CFRP) composite is the material of choice in aerospace industry due to its superior strength to weight ratio, high stiffness, corrosion resistance, etc. Percentage of usage of different types of composites in commercial aircrafts has been continuously increasing. Number of parts made from composites has increased from year to year and can be seen in Fig. 1.1. Now a days, CFRP laminates have found wide applications in many other areas such as automotive, marine, sports, civil structures, etc. These structures or components experience various complex loading conditions across their service life which greatly affects their failure behaviour. Unlike conventional metals, composites have very poor compressive strength and high tensile strength. Interlaminar shear strength (ILSS) is another weakness in case of layered composites. These limitations of composites can cause serious damages under transverse bending loading conditions. It induces interlaminar shear stress which causes delamination opening. Furthermore, it promotes a drastic reduction of the bending stiffness of a composite structure. Compressive stresses on one side of the structures present due to flexural load can lead to local buckling.

It becomes more severe when structures have open cut outs because they act as stress raisers. Since the structures like wing of an aircraft and hull of a marine ship have multiple cut outs for assembly purpose or electric wiring purposes, their behaviour and failure mechanism are very different from the one without cut outs. Therefore, it is important to analyse the structures having cut outs under flexural loading conditions. Also the damage mechanics in composites with interacting failure modes like matrix cracking, fiber breakage, debonding and delamination is very complex phenomenon. Accurate prediction of the damage behaviour of composite laminated structures can lead to the effective and sustainable design of structures. However, several onset interacting failure modes stated above and their inherently brittle, inhomogeneous and anisotropic nature causes lots
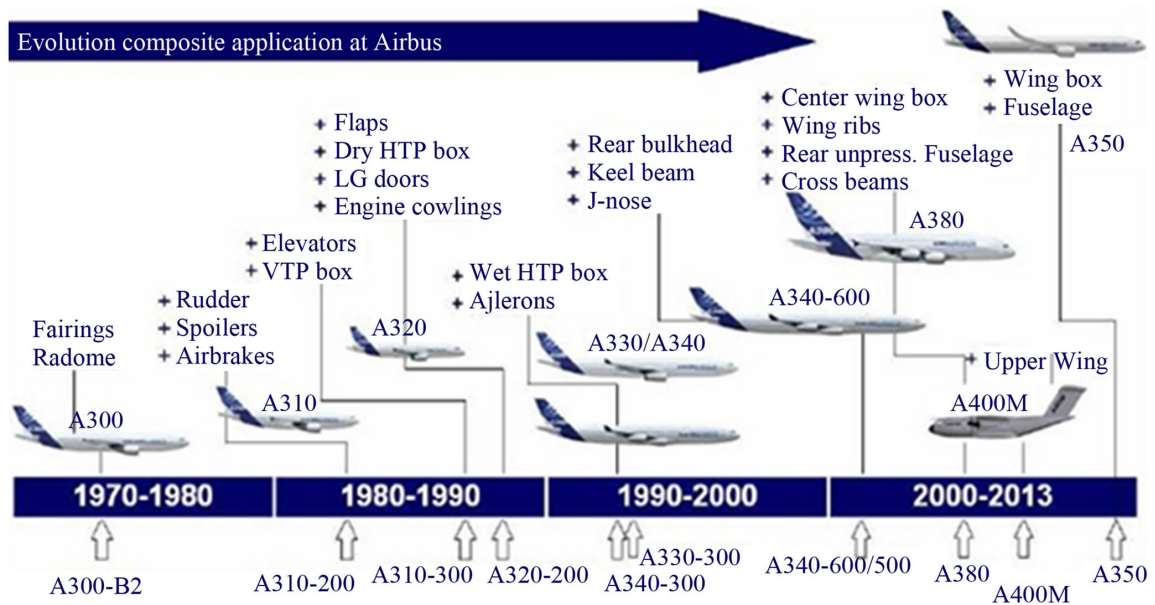
Figure 1.1: Schematic of usage of composite in various parts of commercial aircrafts [1]

of problems. This can be done through FEA based progressive failure analysis (PFA). It facilitates the simulation of degrading structural response and helps in developing the damage tolerant design which is a prime concern in aerospace industry.

1.2   Literature review

Many researchers have studied the effect of flexural loading on different composites. The flexural study can be extended to study the interlaminar shear effects and buckling also. The interlaminar fracture toughness of the laminates can also studied through various configurations of flexural loading. The present study is extended to failure analysis of composite under flexural loading. Failure analysis is a crucial element in damage tolerant design concept. A brief literature review about the flexural study of composites which covers experimental, analytical and FEA outcomes, is presented in the following section. Subsequently, various findings of failures in composites are briefed.

1.2.1   Flexural study of composites

The failure analysis of composite laminates subjected to out of plane load causing bending has not received as much attention as in-plane loading. Kedward [3] used short beam test method under three point bending to estimate ILSS. He showed that beam geometry, material properties and laminate construction dramatically influence the distribution of stresses over the beam width. Chen et al. [4] investigated the elastic-plastic response of interlaminar stresses in composite laminates due to bending and torsion using the finite element method. The plasticity model used is a general three-dimensional orthotropic yield criterion, which is quadratic in stresses, in conjunction with incremental flow theory. Wisnom [5] analysed effect of specimen size on the bending strength of unidirectional Carbon fibre-epoxy. He suggested a reduction in compressive strength with specimen size which may be even larger than the reduction in tensile strength. Reddy and Reddy [6] devel-

2

oped finite element computational procedure to find linear and non-linear first-ply failure loads of composite laminates subjected to in-plane and transverse loads. Cui and Wisnom [7] introduced a combined stress-based and fracture mechanics based models for predicting delamination in composites. It is able to predict the onset and growth of delamination very well in case of three point bending with cut central plies.

Echaabi et al. [8, 9] have presented theoretical and experimental study of damage progression and failure modes of graphite-epoxy laminates in three points bending tests and also compared different failure criteria. Padhi et al. [10] presented a method to study the non-linear behaviour of laminated composite plates with subjected to transverse pressure. They used Hashin's and Tsai-Wu's failure criterion to predict the failure mechanisms. Dufort et al. [11] have used grid technique to show the warping of cross section of composites in three point bending and compared with higher order theories of plates and beams of composites. Feraboli et al. [12] investigated the correlation of ILSS test of uni-directional laminates to multi-directional ones. Bosia et al. [13] have studied through-the-thickness deformation of laminated composite plates subjected to out-of-plane line and concentrated loads experimentally and numerically with various span to thickness ratios. Turon et al. [14] proposed thermodynamically consistent damage model for the simulation of progressive delamination in composite materials under variable-mode ratio. Mulle et al. [15] have carried out stress-strain analysis of composite structures having central reinforced zones under three and four point bending using fiber bragg grating (FBG) sensors and 3D digital image correlation (DIC). Santiuste et al. [16] compared Hou and Hashin criteria under dynamic conditions, analysing the failure of beams subjected to low-velocity impacts in a three point configuration. Ernst et al. [17] carried out multiscale failure analysis of textile composites and simulated three point bending as a macroscale exmaple and compared with experimental results. Ullah et al. [18] addressed multiple delamination in CFRP laminates under bending. They reported that top and bottom layer fail due to mode-I type of failure while the mid-layers fail due to mode-II type. Recently, Makeev et al. [19, 20] have established a method to experimentally characterize composite materials through short beam method using DIC technique.

1.2.2 Failures in composites

To utilize the high potential strength of FRP composites, it is essential to study the failure mechanism thoroughly. That includes fiber failures, inter fiber failures, interlaminar failures, etc. It is necessary to relate the different failure modes to micro-level to simulate material response at macro-level. To get the response of the components under different loading conditions experimentally is time consuming and expensive and sometime it is not possible at all. Failure analyses through FEM can help upto some extent to predict the behaviour of composites but it needs failure criteria which provides accurate and meaningful predictions of failures. Puck [21] and Hashin [22] have come up with the criteria for FRP composites which are based on failure mechanism. Hashin's criteria is the fit of quadratic stress invariants to the experimental results. However, Puck's criteria is based on the physics of the failures occurred in composites.

Later many researchers like Tsai [23], Hart-Smith [24], Sun [25], McCartney [26], etc. have established failure criteria based on various failure modes. Recently Hinton et al. [27] investigated various failure theories. They conducted many experiments with different FRP composites and loading conditions. The experimental results are compared with leading failure criteria. Pinho et al.

[28] have proposed the failure criteria based on physical models for each failure mode and non-linear shear behaviour of FRP composites.

The above mentioned failure criteria are only applicable to intra-laminar failure modes. Inter-laminar failures like delamination is not included in these failure theories. Through cohesive zone modelling (CZM) between the layers, delamination can be introduced in the failure analysis. Dugdale [29], Barenblatt [30], Hillerborg [31], Tvergaard [32], etc. proposed various cohesive models. Xu and Needleman [33] have proposed exponential and coupled cohesive law for FEA. Usually cohesive models have mesh dependency and so mesh size effects inherently plays role in delamination for composites. Turon et al. [34] have proposed a method to determine cohesive modeling parameters for coarser mesh and easy convergence.

1.3   Motivaion, Scope and objective of the study

Composite materials are being increasingly used in many industrial applications thanks to their excellent mechanical properties and low specific weight. Understanding the mechanical behaviour of the composites is an important task while designing these structures or applications to get the advantage of composite. Often these composites structures have multiple holes for fastener purpose, access for maintenance, electric wiring or weight reduction, etc. as shown in Fig. 1.2. It is the source of highly localized stress areas. These notches can interact with each other and can cause severe damage to the structures. Composite structures, such as robot arms, drive shafts, and helicopter blades, wings of aircraft should be modelled as beams subjected to loads that undergo mainly flexural loading. Even slightly misalignment in in-plane loading condition or of fiber orientation can produce flexural load in panels. This flexural load produces delamination opening due to induced interlaminar shear stress. This delamination reduces the inherent load carrying capacity of the structures significantly and can not be detected through visual inspection. In addition to that, propagation of damage owing to buckling of delaminated part is one of the critical causes of failure in composite laminates.

The ply-to-ply interface strength of CFRP laminates is very poor. The interlaminar strength is further influenced by layup configurations. So it is very important to know the behaviour of CFRP laminates under flexural loads. Accurate prediction of the damage behaviour of composite laminated structures can lead to the design of efficient structures. This can be done through finite element based progressive failure analysis (PFA). It helps to predict the damage initiation and its growth. Also the behaviour of the structure having open cut-outs can be very helpful for further detailed real time failure study because there is huge possibility of damage initiation from these cut-outs. The placement and arrangements of holes can affect the stress distribution substantially. The effect of spacing between holes on stress concentration factor (SCF) plays crucial role too. Upto the authors knowledge, multiple hole interaction in CFRP panels under flexural loading is not yet studied thoroughly. The objective of the study is to investigate the failure modes, ultimate failure loads, failure initiation and propagation of CFRP panels having single and multiple holes under the flexural loading.

Figure 1.2: Wing structure of Airbus A350 XWB (left) and rear fuselage of Boeing 787 Dreamliner (right) (Source : Airbus Co. and Boeing Co.)

1.4 Thesis layout

The outline of the thesis presented here is as follow:

In chapter 1, basics of composites and its applications are briefly described. Importance of study of flexural behaviour of composite laminates is explained. The scope and objective of the present study is discussed. Various outcomes of flexural study and failure analysis of the composites are presented briefly. The development of different failure theories and modelling aspects of these failures of composites are also reviewed in brief.

Chapter 2 is entitled for experimental characterization of CFRP laminates for flexural and fracture toughness in mode-I (DCB test) and mode-II (ENF test). These tests are carried out as per the ASTM standards. The specimen fabrication method and experimental setup for each test are mentioned. DIC method is explored to measure the fracture toughness without measuring delamination length compared with other methods.

Chapter 3 deals with experimental study of damage mechanics of CFRP laminates having different holes configuration under flexural loading. DIC is used to get whole field strain and displacement data in the through-thickness direction along the length. Unidirectional and quasi isotropic laminates are analysed under four-point bending. Load carrying capacity and failure modes in different cases are compared and discussed.

In Chapter 4, the developed FEM model for four point bending is explained. Progressive failure analysis with different failure criteria like Hashin's, Ye's, LaRC04, etc. is carried out for CFRP laminates. Also delamination through CZM is implemented. The calibration of CZM properties is also carried out and discussed. The interaction between the holes under flexural loading is studied further. The results of PDM predictions are compared with experimental one.

Chapter 2

Experimental characterization of CFRP for flexural and interlaminar fracture toughness properties

2.1   Introduction

It is essential to characterize the material properties of composite for further usage like FEA. These material properties are inputs for it and depends on them to get the accurate and exact results. In the present work, the flexural properties and fracture toughness (mode I and mode II) of unidirectional CFRP are measured which are used further in PDM and CZM modelling. Flexural modulus and strength are not the primary material properties. Though flexural loading is the resultant effect of induced tensile, compressive and shear loading, the real flexural loading is different than these in-plane loading. It is necessary to simulate the real flexural loading in FEA. This flexural modulus will replace the axial Young's modulus along which flexural loading produces tensile or compressive stress state. To model the interfaces between the layers during flexural loading in FEA, mode-I and mode-II fracture toughness are required as an input. Therefore, mode I and mode II fracture toughness tests, double cantilever beam (DCB) and end notched flexural (ENF) tests respectively are conducted for CFRP composites. Physics based failure theories such as Puck's, LaRC04, etc. are based on the fracture toughness of the composites to evaluate the damage in the structures. Fracture toughness is an important parameter for CZM which is traction-separation law for interfaces between the layers. The area under this traction-separation law is equivalent to fracture toughness of the interface in composites. Other parameters of CZM can be derived from fracture toughness. The failures like delamination and debonding can be modelled.

2.2 Flexural properties CFRP composites

2.2.1 Standard test methods

There are many standard test methods for flexural established by various national and international standardization bodies such as ASTM-D790, ASTM-D6272, ASTM-D7264, ISO 14125, EN 2562, etc. The standard followed in the present work is ASTM-D7264. Span-to-thickness ratio plays a major role in the behaviour of composite during flexural test. Shear effects are significant in short span-to-thickness ratio. To exclude these shear effects, span-to-thickness ratio is kept 32:1 as opposed to 16:1 in ASTM D 790 test method. ASTM D 7264 is to evaluate long-beam strength in flexural loading. Three- and four- point loadings are included in the standard. A flat rectangular specimen is simply supported near to its ends and loaded centrally in three-point bending. Similarly, it is simply supported to its ends and two loads placed symmetrically between the supports for four-point bending. Both loading conditions have their individual benefits and applications. To obtain local stress concentrations and additional shear effects, three-point bending is used because it induces maximum bending moment at the center loading point with shear force uniform throughout the span length except the center loading point. That is the reason why three-point flexural loading is used to study shear effects in short-beam specimens. Four-point loading is useful when pure bending moment between the loading points is required. The shear force will be identically zero and bending moment will be uniform in this region. In the present work, the focus of the study is pure flexural loading. Therefore, all flexural tests are carried out on four-point bending fixture.

2.2.2 Specimen fabrication

The CFRP laminate sheets are prepared from unidirectional carbon fiber mat (Goldbond® make) of 230 gsm weight through hand-layup technique. The matrix composed of epoxy resin LY-556 and hardener HY-951(Huntsman) in proportion of 10:1 by weight. After layup, curing is done at room temperature for 24 hrs. From this laminate, flexural test specimens are accurately machined to the exact dimension on a table circular saw machine. The specimen is made up of 16 UD layers having layer thickness of 0.321 mm. Span-to-thickness ratio is kept 32:1 and total length of specimen is kept 20% longer than span length. The derived length is 220 mm and width of the specimen is kept 13 mm as suggested in the ASTM-D7264. A random speckle patterns are made over the thickness side to perform DIC analysis. First, the thickness side of the specimen is cleaned with isopropyl alcohol. Then Asmaco® spray paint of white colour is applied over the surface and allowed to dry for an hour. The speckles are generated with GOLDEN® acrylic paint of carbon black color (# 8040-Series NA) and Iwata CM-B airbrush having 0.5 mm nozzle diameter. The speckle distribution should be random to get the accurate DIC results.

2.2.3 Experimental setup

Experimental setup used for flexural test is shown in Fig. 2.1. The test is carried out on computer controlled MTS Landmark® servo-hydraulic cyclic test machine having capacity of 100 kN. A 2D-DIC system (from Correlated Solutions, Inc.) is used to get the displacement and strain data. It has single Grasshopper® CCD Camera (POINTGREY - GRAS-50s5M-C) with resolution of 2448×2448 pixels^2 coupled with Schneider Xenoplan lenses of 35 mm focal length. It is mounted on the tripod.
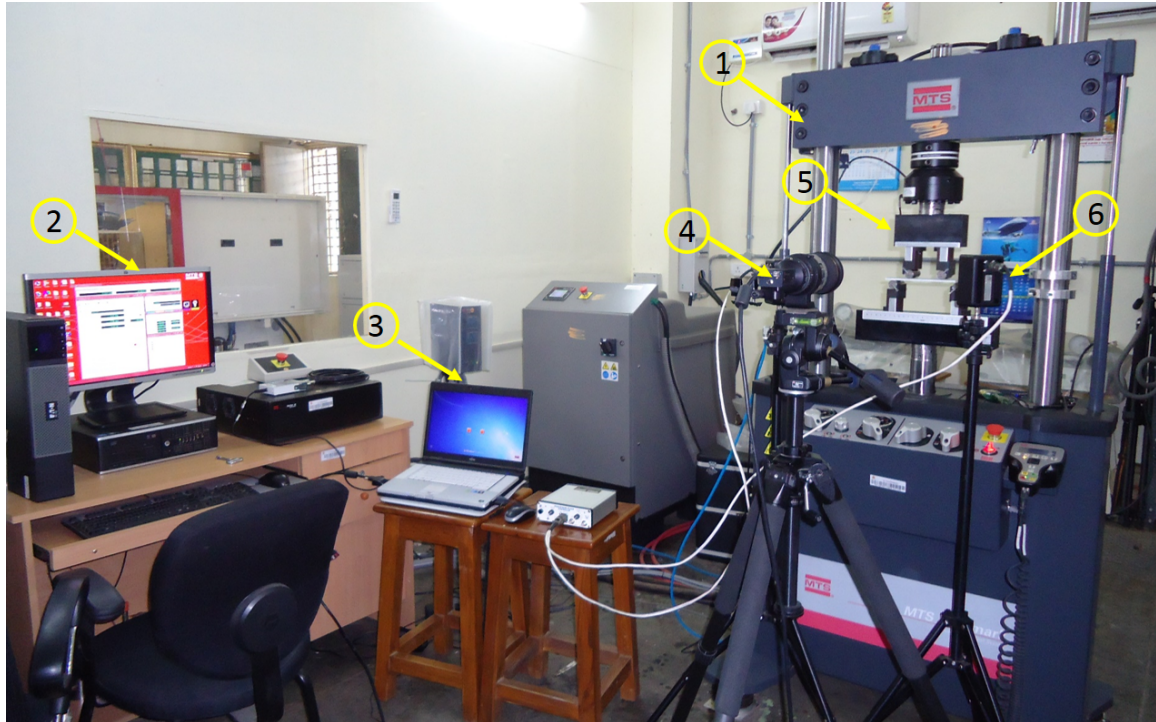
1. MTS machine	2. MTS controller PC	3. Image grabbing PC
4. DIC camera	5. Bending fixture	6. LED light source

Figure 2.1: Experimental setup for flexural test

The horizontal level of camera is ensured through inbuilt spirit level. The camera is properly aligned with the specimen so that it can capture the image of the specimen without any inclination. Two white LED (Light emitting diode) light sources having 30 W capacity are used on both sides of the camera to ensure proper illumination on the specimen surface. Aperture of the length is tuned to adjust the depth of the field to get the fine field of the view and to avoid the saturation of the pixels over the field of view. Camera is connected to the laptop pre-installed with Vic-Snap 2009 software (from Correlated Solutions, Inc.) used for grabbing the images. A data acquisition card (DAC) from National Instruments is connected to this laptop that interacts between MTS controller and the laptop to store the load-displacement data for each image grabbed by the camera during the experiment. The first image is taken initially at zero load called reference image. All the calculations of displacement and strain will be carried out with respect to this image in DIC post-processing. The frequency of image grabbing is kept 10 Hz. Four-point bending fixture is used for the test and span length is kept 170 mm. The fixture has four rollers with diameter 25 mm. The load span is kept half of the support span and placed symmetrically between support rollers. The experiment is performed under displacement control mode. The displacement rate is kept 1.0 mm/min as suggested in the ASTM-D7264. The axis of the loading and support rollers are checked for parallelism and aligned properly. Vic-2D software (from Correlated Solutions, Inc.) is used for post-processing the images to get the maximum strain and the deflection of the specimen at the center of the support span.

2.2.4 Results and discussion

The maximum flexural stress and strain at any given point occurs at the outer most surface and plotted in Fig. 2.2b. The deflection at central point is measured through DIC is used for load-deflection data (plotted in Fig. 2.2a). The flexural modulus of CFRP panel can be calculated from this load-deflection data [35]. It is compared with the value got from DIC data and given in Table 4.2.

$$\sigma = \frac{3PL}{4bh^2} \tag{2.1}$$

$$\varepsilon = \frac{4.36\delta h}{L^2} \tag{2.2}$$

$$E_f^{secant} = \frac{0.17L^3 m}{bh^3} \tag{2.3}$$

where,

σ = stress at the outer surface in the load span region, MPa

ε = maximum strain at the outer surface, mm/mm

δ = mid-span deflection, mm

P = applied force, N

L = support span, mm

b = width of beam, mm

h = thickness of beam, mm

m = slope of the secant of the force-deflection curve

(a) Load-deflection curve   (b) Stress-strain curve for flexural test
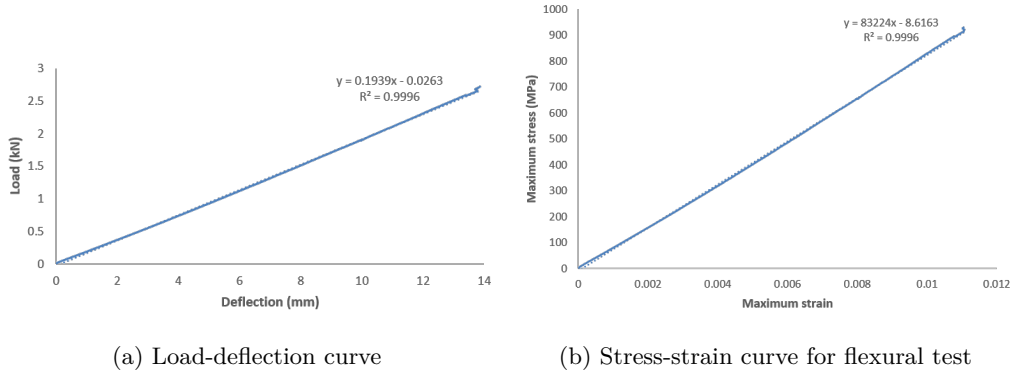
Figure 2.2: Experimental results for flexural test from (a) MTS and (b) DIC

Table 2.1: Longitudinal modulus from flexural test for CFRP panels

Specimen	from beam theory (GPa)	from DIC (GPa)
1	82.46	82.29
2	80.23	80.62
3	83.17	83.58
Mean	81.95	82.16
Std. Dev.	1.53	1.48
CV(%)	1.87	1.80

2.3 Fracture toughness of CFRP composites

2.3.1 Standard test methods

Delamination is one of the critical failure mode in FRP composites. They are significantly weak interlaminar fracture properties. One way to study and analyse delamination in composites is through fracture mechanics but it needs interlaminar fracture toughness properties of composites. It helps to establish delamination failure criteria for damage tolerance and durability analyses. ASTM has formed various standard test methods such as D5528, D7905 and D6674 for various fracture modes. Mode-I interlaminar fracture toughness of CFRP is measured using double cantilever beam (DCB) as per ASTM-D5528. Similarly, end-notched flexure (ENF) test is performed to find mode-II fracture toughness as per ASTM-D7905. These tests are only applicable to carbon-fiber and glass-fiber reinforced composites. Furthermore, it is limited to only unidirectional layup sequence. These tests cannot be extended for mode-III. It needs the development of new standard test methods. DCB and ENF tests are are pure mode-I and mode-II testing respectively. However,real structural applications undergo combination of these two modes. Therefore, tt can affect and behave very different in various mixed-mode loading conditions as compared to the pure-mode loading. This promotes to establish the test method through which resultant interlaminar fracture toughness can be determined. ASTM has developed a test-standard D6671 for this purpose. It is mixed-mode bending (MMB) test. It also limited to unidirectional CFRP laminates.

2.3.2 Pure mode-I DCB test

Specimen fabrication

The fabrication technique and material used for making the laminates are the same used earlier in flexural test (refer Sec. 2.2.2). The laminate is made up of 12 unidirectional layers. A polyester film having thickness of 45 μm is used as an insert in the mid-plane that serves as a delamination initiator. It is to be noted that the maximum thickness recommended in D5528 is 13 μm. The width of the film is 50 mm. It is inserted at mid-plane during the layup. The length, width and thickness of the DCB specimen are 125 mm, 25 mm and 4 mm respectively. After cutting the specimens as per the given dimensions from the laminates, hinges are bonded to the end where insert is kept (see Fig. 2.3). The adhesive used is Araldite 2011 manufactured by Huntsman. It cures at room temperature. Random speckle pattern is generated on the thickness side for displacement measurement through DIC.

Experimental setup

Since DCB specimen is taking around 100 N maximum so performing the test on the machine having load-cell of 100 kN is not a good practice. The test is performed on computer controlled Instron® 5966 electromechanical universal testing machine having capacity of 10 kN. 2D-DIC system is also used here to track through the thickness full displacement and strain field. The lens used here is Tamron lens (Model: SP AF 180 mm F/3.5 Di). The machine has not the facility to connect NI DAQ card to extract the load data from machine so triggering of the machine and DIC system is done manually and proper care is taken to minimize the time lag and trigger both things simultaneously. Other configuration of the setup is as same as flexural test. The displacement rate is kept 2.5
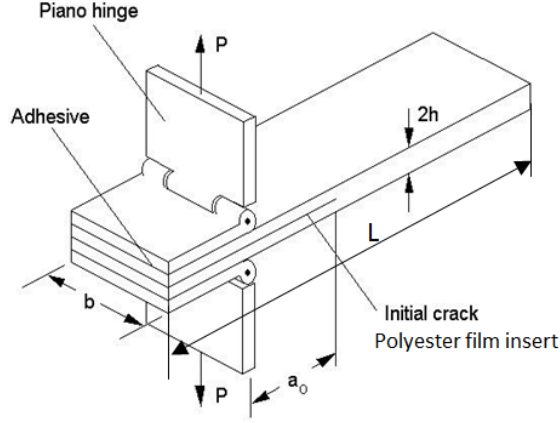
Figure 2.3: Schematic of DCB specimen

mm/min. The load-displacement extraction rate is kept 10 Hz in loading machine and DIC as well. The test is stopped after delamination propagates significantly to get the sufficient data after crack initiation. The delamination should be propagate uniformly throughout the width and the same should be observed throughout the test.

Results and discussion

The fracture toughness of mode-I can be calculated through modified beam theory (MBT) method [36]. It is derived from comparing the strain energy release rate and energy consumed in delamination propagation.

$$G_{Ic} = \frac{3P_{max}\delta}{2ba} \tag{2.4}$$

where,

P_{max} = maximum load

δ = load point displacement

b = specimen width

a = corresponding delamination length

One problem in the method is that delmination length has to be measured accurately which is very difficult. There are methods to find mode-I ERR that does not require to measure delmination length [37, 38]. Through Timoshenko beam theory, J-integral can be calculated without measuring the delamination length which is equal to the mode-I fracture toughness within the frame of linear elastic fracture mechanics (LEFM).

$$G_I = \frac{2P\theta_m}{b} \tag{2.5}$$

where,

P = load at the end of DCB

θ_m = total rotation at the end of DCB

Through DIC, the displacement is extracted. Two appropriate points at the end of the DCB are selected and corresponding displacement and coordinates are extracted from DIC (see fig. 2.4).

11

Total rotaion is calculated with the DIC data as follows :

$$\theta_m = \frac{1}{2}\left(\frac{\partial u}{\partial y} - \frac{\partial v}{\partial x}\right) = \frac{1}{2}\left(\frac{u_A - u_B}{y_A - y_B} - \frac{v_A - v_B}{x_A - x_B}\right) \quad (2.6)$$
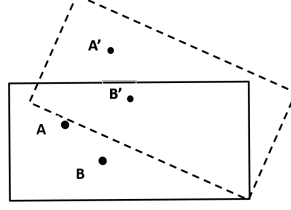
Figure 2.4: Schematic diagram showing one end of DCB specimen

The load-displacement curves for different specimen are plotted in Fig. 2.5a and mode-I fracture toughness is also plotted versus displacement in Fig. 2.5b. The comparison of mode-I fracture toughness measured from MBT method and DIC is given in Table 2.2.

Figure 2.5: Experimental results of DCB test

(a) Load-displacement curve

(b) Mode-I ERR vs. displacement
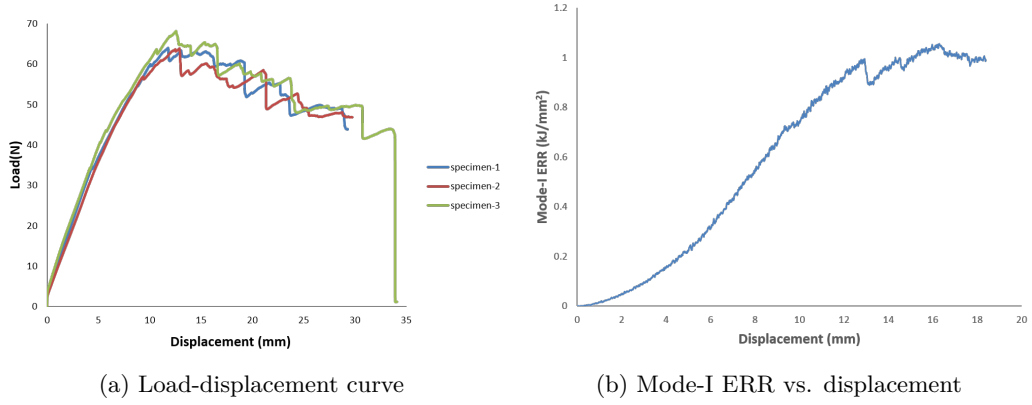
Table 2.2: Mode-I fracture toughness for CFRP panles

Specimen	from MBT (kJ/m^2)	from DIC (kJ/m^2)
1	1.14	1.1
2	1.05	1.0
3	1.02	1.0
Mean	1.07	1.03
Std. Dev.	0.06	0.06
CV(%)	5.84	5.59

2.3.3 Pure mode-II ENF test

Specimen fabrication

The specimens are made with same procedure as mentioned in Sec.2.3.2. The length and width of the specimen are kept 165 mm and 25 mm respectively. The laminate is made of 12 layers unidirectional.
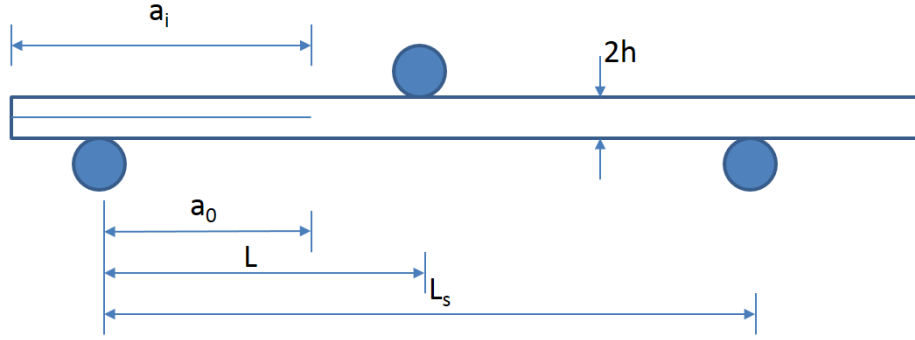
Figure 2.6: Schematic of ENF specimen

The insert length is 50 mm.

Experimental setup

ENF test performed with the same experimental setup used for flexural test (see Fig. 2.1). Three-point bending loading condition is used instead of four-point bending. The span length is 100 mm and the loading roller is kept at the center i.e. it is 50 mm away from each support roller (see fig. 2.6). The displacement rate is kept as 1 mm/min. The load-displacement extraction frequency is kept 10 Hz in loading machine and DIC system. The test is performed for two cases which are precracked (PC) and non-precracked (NPC). When delaminaton starts propagating from preimplanted insert then the the fracture toughness value calculated is called non-precracked fracture toughness. If the delamination starts from well ahead from the insert then it is called precracked fracture toughness. In each of case, there is need to determine the compliance for calculation of fracture toughness so compliance calibration is carried out to get the accurate compliance. These all cases can be performed on a single specimen itself. First non-precracked test is carried out. The specimen is placed on the fixture such that the delamination front is 20 mm away from one of the support rollers and start loading the specimen. It should be continued maximum upto the half of the maximum load it can take so that delamination cannot propagate but compliance can be calculated from the linear load-displacement curve. Again the same test procedure is performed with delamination front kept 40 mm away from the support roller. Rearrange the specimen so that the delamination front is 30 mm away from support roller and load the specimen until delamination propagates significantly and load starts decreasing. The compliance should be calculated again and maximum load and corresponding displacement of loading roller are noted. The advanced delamination front is marked and is checked whether delamination is propagated uniformly throughout the width. Non-precracked fracture toughness is calculated from the extracted data from the test. Precracked test is performed in a same way as above with the advanced delamination front.

Results and discussions

The load displacement curve for a specimen is shown in Fig. 2.7a for different cases. Mode-II fracture toughness can be calculated using compliance calibration (CC) method. It is assumed here that the compliance is proportional to the cube of delamination length (see Fig. 2.7b). G_{IIc} will be the minimum of the values calculated for PC and NPC cases. It is to be noted that compliance in FNF

is proportional to the cube of delmination length. Compliance of ENF in each case is calculated for different delamination length i.e. 20, 30 and 40 mm. From that fracture toughness can be calculated as per Eq. 2.7 [39]. The mode-II fracture toughness for PC and NPC are listed in Table 2.3.

$$G_{IIc} = \frac{3mP_{max}^2 a^2}{2b} \tag{2.7}$$

where,

P_{max} = maximum load

a = corresponding delamination length

b = width of ENF specimen

m = CC coefficient determined from fitting a curve of compliance C and delmaination length a, $C = A + ma^3$
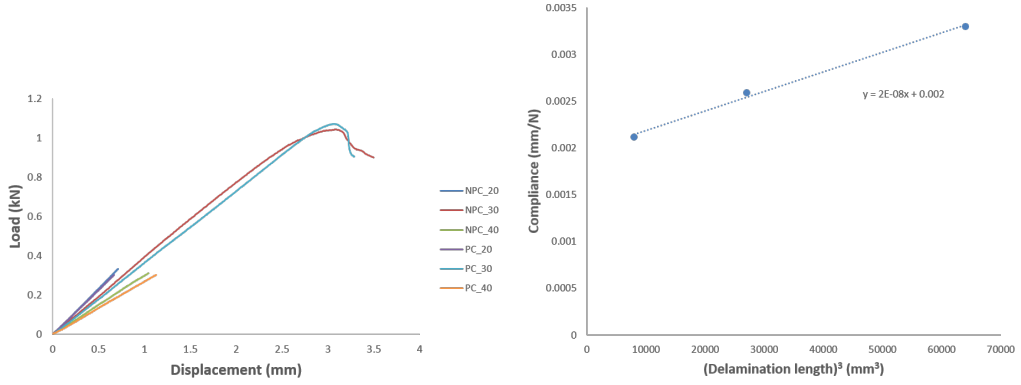
(a) Load-displacement curve   (b) Compliance vs. cube of delamination length

Table 2.3: Mode-II fracture toughness for CFRP panels

Specimen	NPC (kJ/m^2)	PC (kJ/m^2)
1	1.35	1.26
2	1.23	1.19
3	1.27	1.21
Mean	1.28	1.22
Std. Dev.	0.06	0.04
CV(%)	4.76	2.96

2.4 Closure

In this chapter, flexural modulus of UD CFRP panel is found out using DIC. Flexural modulus is found out to be 81.95 GPa which is slightly lower than the longitudinal Young's modulus (84.16 GPa) from tensile test. Method to find mode-I fracture toughness without measuring delamination length is successfully implemented through DIC. In this method, J-integral is calculated from load and total rotation at the end of DCB specimen. That is equal to mode-I ERR within the frame of LEFM. The value is in good agreement with the one determined from MBT with help of delamination length. Mode-I ERR is found out to be 1.03 kJ/m^2. Similarly, ENF test is performed to find mode-II

fracture toughness. It is calculated through CC method. It is found out that mode-II ERR in case of NPC test comes out to be higher than that of PC test. Therefore, value of mode-II ERR in PC test is used for further application which is 1.22 kJ/m^2. There are some challenges and issues to be discussed in fracture toughness tests. Firstly, The recommended thickness for the insert for initial delamination should be less than 13 μm. The insert used in the fabrication of the specimens has thickness of 45 μm approximately. The effect of the insert thickness on the fracture toughness value is not studied. Secondly, DCB test is performed on the machine having 10 kN loadcell and the maximum load taken by DCB specimen is less than 100 N. Error in load data can significantly affect the mode-I ERR value. Thirdly, The difference between mode-I ERR and mode-II ERR is quite less. The reason behind this is still not known.

Chapter 3

Experimental study of damage mechanics of CFRP laminates in flexural loading

3.1 Introduction

Composites are widely accepted across many applications but understanding the stress strain distribution under different loading conditions is still not completely understood. Among these applications, composites panels have multiple holes for fastener purpose, access for maintenance, electric wiring or weight reduction, etc. It creates notches in the laminates that act as stress raisers. Study of these notched laminates is important because damage may initiate and propagate from these areas. Especially, when there are multiple holes in close proximity, they interact with each other and also edge effects come into the picture if holes are near to edges. In these conditions, the size and the placement of the holes become critical. In this study, four different types of holes configuration is analysed keeping in view the alignment and the placement of the holes. They are as follow : a) Single hole (1H) and the rest are multiple holes created in different directions : b) Longitudinal (2HL) c) Transverse (2HT) and d) Diagonal (2HD) (inclined 45°) as shown in Fig. 3.1. To these several configurations, flexural loading is applied. Composites are orthotropic material and in addition to that, they have different characteristics in tensile and compressive loading. They may have different strengths, Young's modulus, poisson's ratio in pure compression and pure tension load. Studying these two combined loading conditions is more important than doing the same individually because the structural applications often come under the various mixed mode loading. The flexural loading is one of the example in which some layers of the composites come under tensile load and the other under compressive. Moreover, it includes interlaminar shear loading in which layered composites are very weak. CFRP panels are studied with two stacking sequences. First one is unidirectional and second one is quasi isotropic with $[45/0/\text{-}45/90]_{2S}$. Unidirectional laminates are of special interest if structure is going to bear load in only particular direction because unidirectional laminates with fiber direction in that loading have high strength and at the same time reducing the weight of the structure compared to one made with conventional materials. These unidirectional laminates are

weak in other directions. In general practice, quasi isotropic laminates are used if structure comes under loading from all directions. Each layer of quasi isotropic laminates has different mechanical and thermal properties in each direction because each layer properties are dependant on fiber direction. These causes severe interlaminar shear stresses in the laminates. Delamination may initiate and propagate during the severe loading.
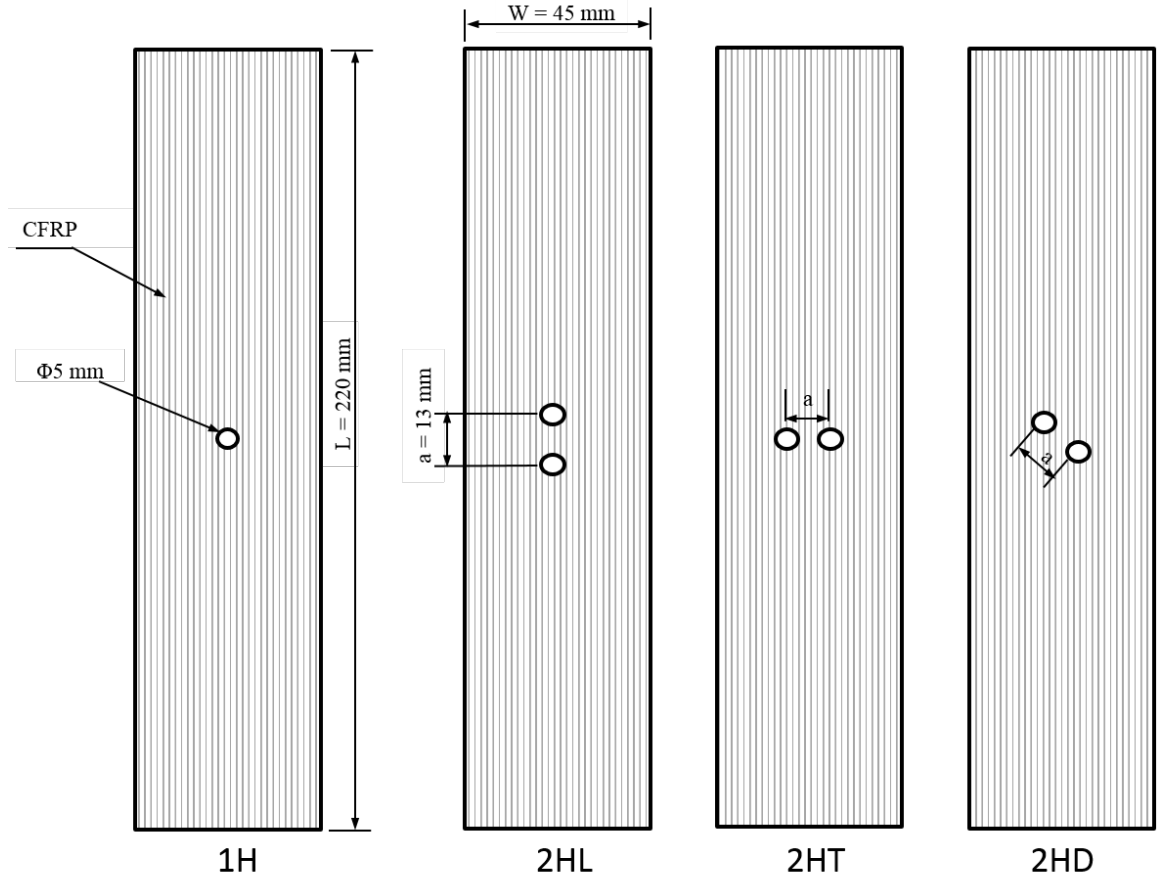
Figure 3.1: Schematic of CFRP panels having multiple holes

3.2   Specimen fabrication

Same material and fabrication technique mentioned in Sec. 2.2.2 is used to make the specimen for this study. Carbon fiber is cut from the fiber mat in $250 \times 250 mm^2$ dimensions with required fiber orientation. The specimen is made up of 16 layers having thickness of 0.333 mm. After the curing of laminates, specimens are cut to the approximate dimensions with table saw and finishing is done with emery paper. The layup sequence in case of quasi-isotropic panels is chosen as $[45/0/\text{-}45/90]_{2S}$. Since flexural stress will be higher at the outer-most layers, keeping 0° layer as much outside as possible will increase the flexural strength of the CFRP panel. Sometime there is possibility to damage the outer layer due to the impact. In this case, it will be very critical to put 0° layer outermost. That is the reason first layer is chosen 45° and the second inside layer as 0° layer to serve

both purpose : high load carrying capacity and protection of 0° layer from impacts. The specimen length and width are kept 220 mm and 45 respectively. 5 mm diameter hole is chosen to avoid the interaction of the hole with edge ($W/D > 3.5$). In two hole configuration, three configurations are tested for flexural loading. The distance between the holes is kept 13 mm to get the sufficient interaction between holes($a/D = 2.5$). Holes are drilled on milling machine with the help of SECO tools at speed of 250 rpm. Wooden plates are used at the side and bottom of the specimen to avoid any damage to the specimen during machining. After fabrication, speckle pattern is produced on the thickness side of the specimen to study the delamination or edge interaction of hole during the flexural testing if present.

3.3 Experimental setup

PDM study is carried out using the same experimental setup used earlier for flexural test. The span length of 170 mm is fixed on bending fixture. The span-to-thickness ratio is maintained 32:1. the loading rollers are 85 mm away from each other and placed at the center such that the symmetry of the four-point loading condition is preserved. The experiment is performed under displacement control mode. the displacement rate is kept 1.0 mm/min and load-displacement data extraction rate is fixed to 10 Hz.
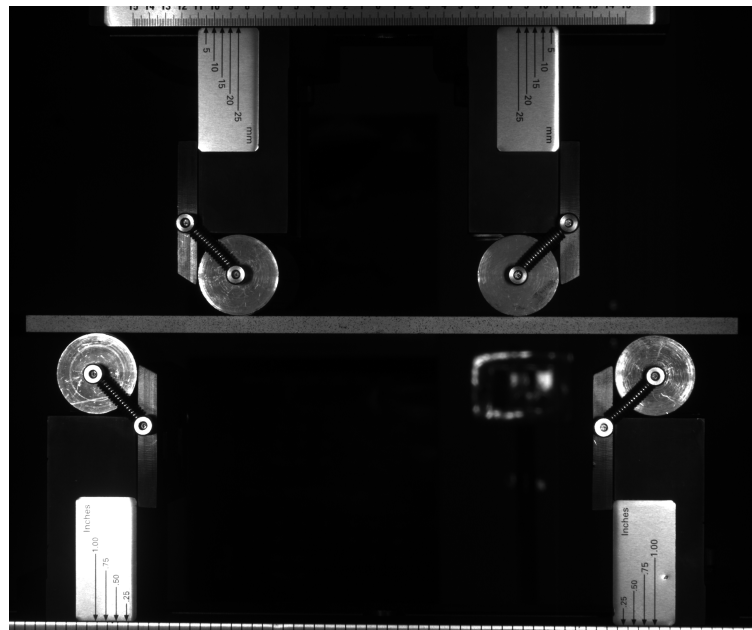
Figure 3.2: Four-point bending fixture with specimen

3.4 Results and discussions

Experiments are carried out for failure analysis of CFRP panels (unidirectional $[0]_{16}$ laminate) under flexural loading. Through-the-thickness longitudinal strain distribution is captured with the help of DIC system to observe the edge effect along the length. It is observed that there is no edge

effect appeared on the thickness side due to holes (see Fig. 3.3). In addition to that, the load and displacement of rollers are extracted from MTS machine. The unnotched specimen was tested first to know the full load bearing capacity of the specimen. Then specimens with single and multiple holes with different configuration are tested under four-point bending. A relative comparison is shown in Fig. 3.4.
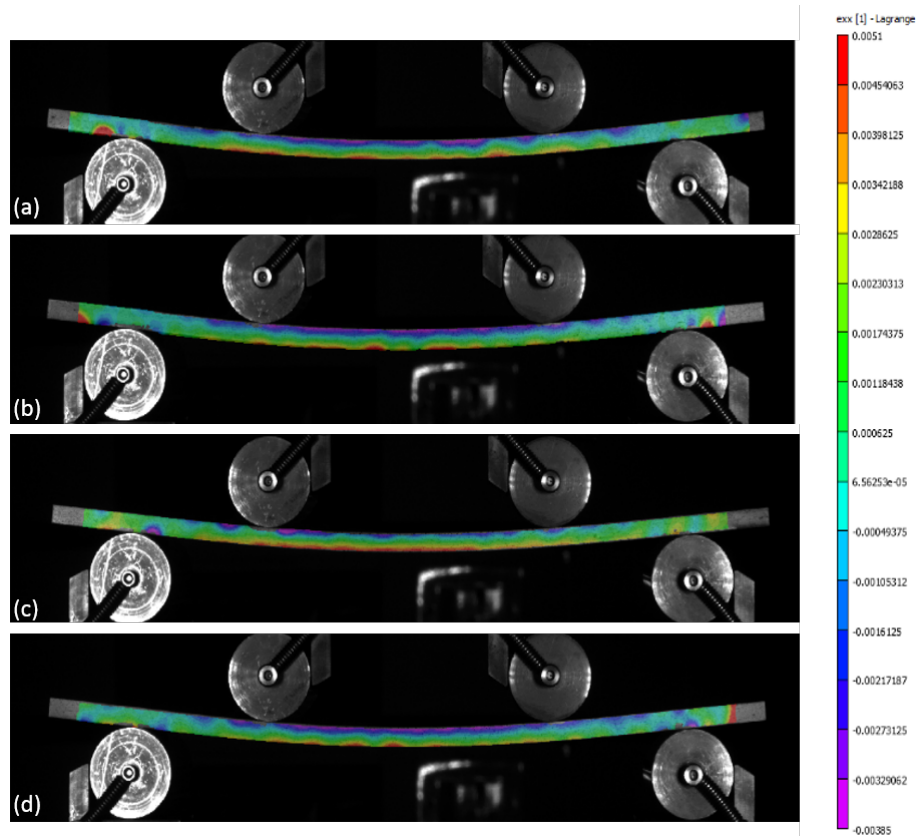
Figure 3.3: Through-the-thickness longitudinal starin in CFRP panels (a) 1H (b) 2HL (c) 2HD (d) 2HT

The damage on different sides at final failure for UD CFRP panels are shown in Fig. 3.5. It is found out that the damage starts on the top-most layer of the panel which is in compressive stress state. The damage at bottom-est layer is observed vary less compared to the top layer. One of the reason behind this happening is the high tensile strength of the CFRP panel compared to compressive one. In all the configurations, damage has propagated in transverse direction passing through holes in the compression side whereas it propagates in longitudinal direction in tension side. Once plies got failed, damage in form of delamination is produced between the layers. It is not that much significant in case of UD because delamination is propagating after the plies have failed so it is like post failure effect.

The layer configuration of quasi-isotropic CFRP panel is chosen as $[45/0/\text{-}45/90]_{2S}$. In the case of quasi-isotropic panel, the edge interaction is not found on the thickness side. The load-displacement curves for different cases are plotted in Fig. 3.6. The damage on different sides is shown in Fig. 3.7 for quasi-isotropic CFRP panels. It is found out that there is no damage detected in the tension side
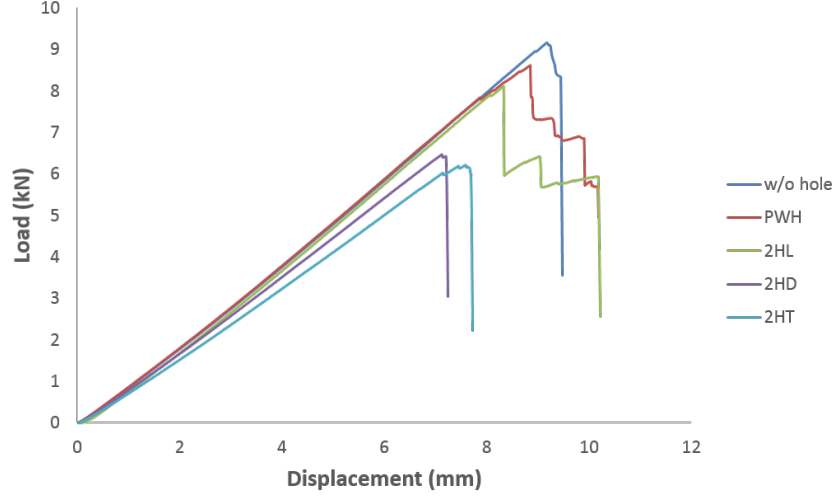
Figure 3.4: Load vs. displacement for UD CFRP panels

of the panels in each case. These layers are still intact. On the compression side, top few layers got damaged and mostly in transverse direction through holes except in 2HD configuration. Damage got propagated in 45° direction through holes. Though the layers on compression side got less damage than those of UD CFRP panels, delaminaton is significantly produced compared to UD panels due to different fiber orientation.

3.5 Closure

Experimental study of CFRP panel having open cutout is carried out under flexural loading. UD and quasi-isotropic panels with single and multiple holes of different configurations are tested and compared with each other. Ultimate load and corresponding displacement of rollers are noted down in Table 3.1. Panel with 2HL configuration is found out to be the best with high load carrying capacity among the panels with multiple holes.

Table 3.1: Experimental results of CFRP panel for flexural loading

	UD		Quasi	
	Ultimate load (kN)	Displacement (mm)	Ultimate load (kN)	Displacement (mm)
Unnotched	9.06	9.25	6.00	12.24
1H	8.61	8.84	5.21	9.85
2HL	8.09	8.31	5.12	10.43
2HD	6.41	7.13	4.74	10.32
2HT	6.17	7.6	4.00	8.53

The weakest layer is top-most layer in compression due to poor compressive strength of CFRP panels. The compression side is found out to be the first ply to be failed. Damage is in forms of matrix failure and fiber kinking in compression side. Damage propagates in transverse direction in

| Compression side | Tension side | Thickness side |
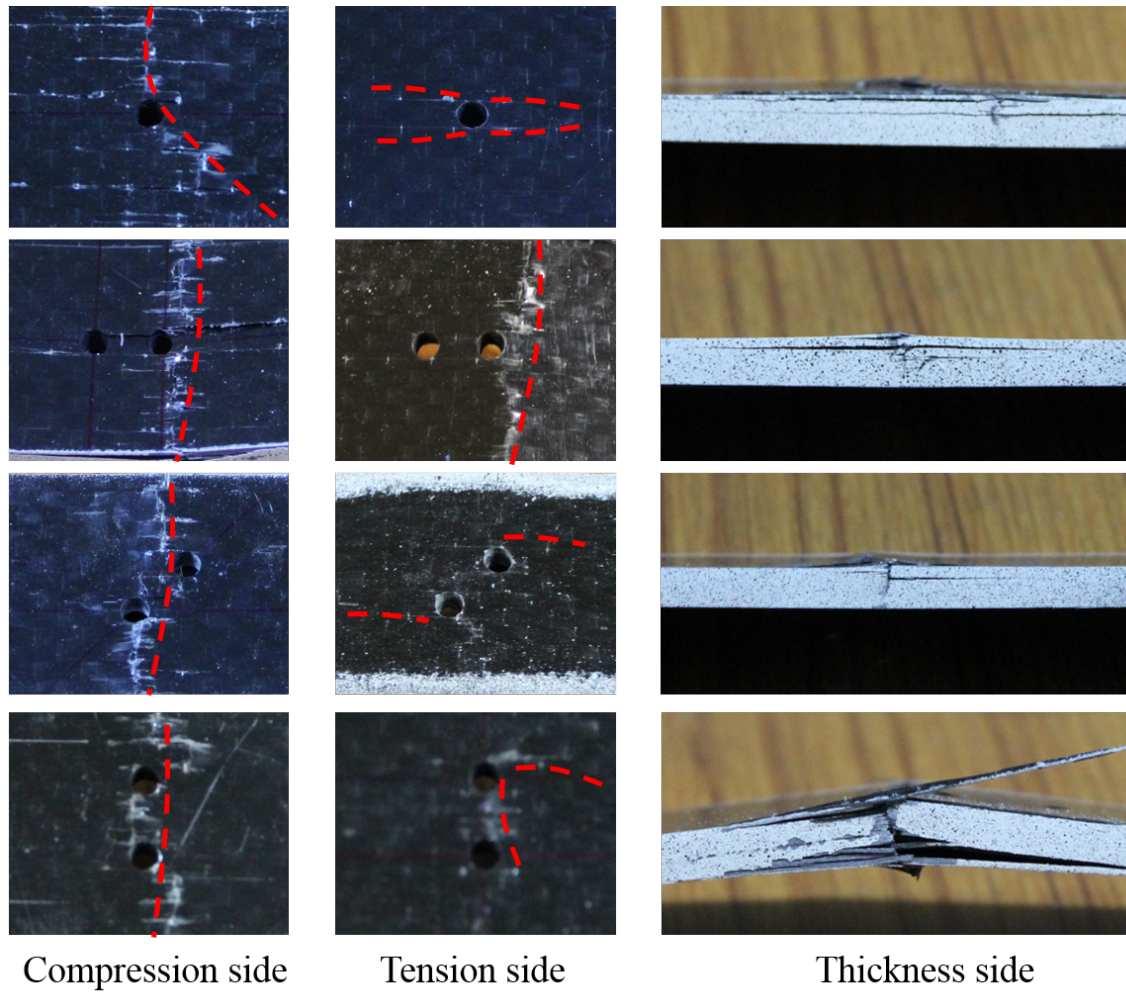
Figure 3.5: Damage in UD CFRP panels

compression side through holes and in longitudinal direction in tensile side originated from holes. There is negligible damage detected in tension side in both layup configuration. Especially, There is no damage detected in tension side in case quasi-isotropic panels. Delaminaton is found out between the layers in compression side.
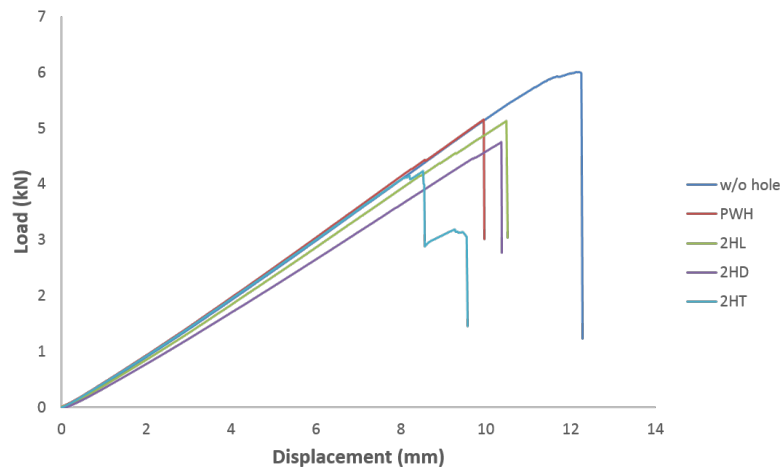
Figure 3.6: Load vs. displacement for quasi-isotropic CFRP panels

Compression side   Tension side   Thickness side
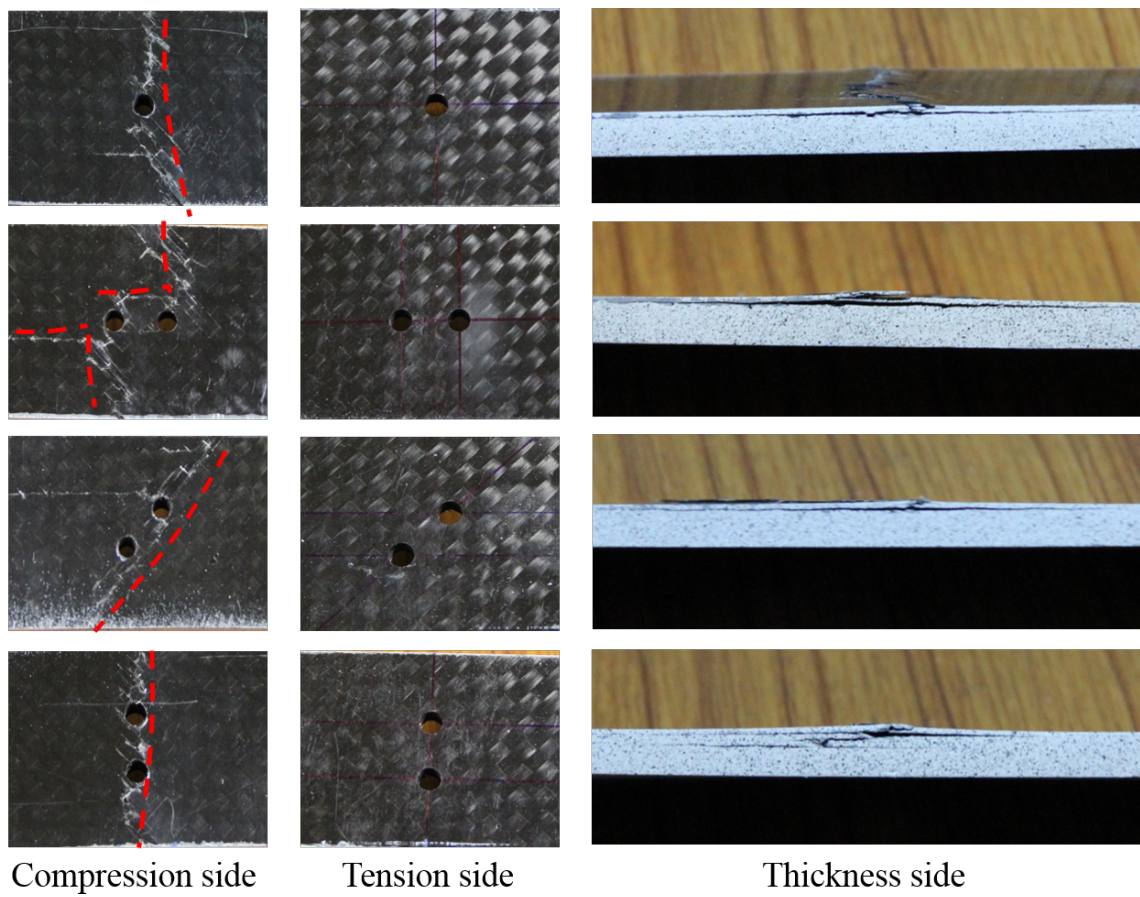
Figure 3.7: Damage in quasi-isotropic CFRP panels

Chapter 4

Progressive damage analysis of CFRP laminates having single and multiple holes

4.1 Introduction

Design of a structure is developed to avoid any failures during the predetermined service life. In conventional metals, cracks are the only failure mode and can be designed components using well-established fracture mechanism. Composites due to heterogeneity and anisotropic nature cannot be studied with the same fracture mechanism. They fall under neither ductile materials nor the classic brittle materials. Moreover, the various damage modes that are interacting with each other makes the damage analysis of the composites more complex. When designing the composite component, two considerations are taken into account : ultimate failure and first ply failure. Structures may bear the load even first ply failure occurs. In general practice, first fly failure is considered more important because it gives somewhat conservative approach in the absence of the physics based failure mechanism for the composites. The failure initiation and propagation in each ply may depend on the constituents used for fabrication, fabrication technique, the stacking sequence, loading conditions, etc. To study the damage mechanics in the structures, performing experiments is a costlier, time consuming exercise. Instead of that, a well established and validated progressive damage analysis (PDA) through FEM can enlighten the damage mechanics. It cannot replace the experimental methods but can aid into it by predicting the damage initiation and propagation in the composites. In this study, CFRP laminates with multiple holes are analysed through PDA algorithm. Various failure criteria such as Hashin's, Ye's delamination, LaRC04 are used here to predict the failures and delamination failure is introduced with cohesive zone modelling (CZM).

4.2 FEM modelling of four point bending

3-D finite element model is developed using ANSYS APDL which is commercially available finite element package. Fig. 4.1 shows a meshed 3-D FEA model for the flexural study. SOLID 186,
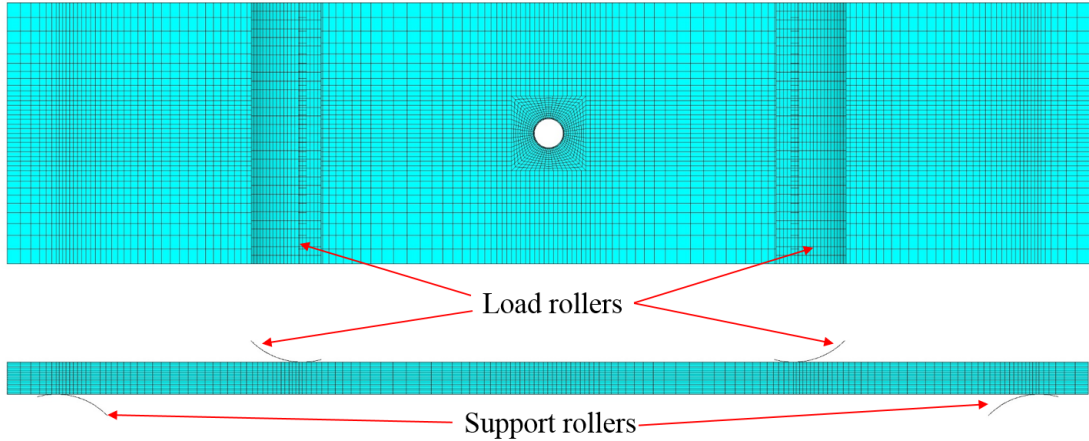
Figure 4.1: ANSYS FEA model for flexural study

a 20 noded brick element is used to model CFRP panel having length of 220 mm and width of 45 mm. This panel has 16 layers of thickness 0.333 mm. In the XYZ coordinate system, length, width and the thickness of the panel are oriented in x, y and z-direction respectively. No. of elements in z-direction is kept same as number of layers in the panel so each element represents a unique layer in the thickness direction. The hole of diameter 5 mm is modelled at the center of the panel. The mesh pattern around the hole is kept finer to capture the high stress gradient near the hole. There are 64 elements generated circumferentially around the hole. Material properties obtained through experimental characterization using DIC are applied to the panel. To simulate four point bending loading conditions, four rollers having radius 25 mm are modelled. Two of those are support rollers and other two are loading rollers. Since the deformation of rollers are not so important, they are kept as rigid bodies. Also to save computation time, only rigid surface of rollers are modelled. Furthermore, The meshing near the contact kept finer to get accurate solution and to avoid convergence issues. Full model is analysed since symmetry may be lost after the damage initiates and propagates further. Fig. 4.2 shows FEA models with different hole configurations.

4.3 Contact parameters

To transfer the load from loading rollers to panel and panel to support rollers, contact pairs are employed in the modelling. The contact analysis is simulated using surface to surface CONTA174 elements along with TARGE170 elements. There are four contact pairs created. Each one is for an individual roller and panel. Each contact pair consists of target surface and contact surface. Surface of rollers is considered as target surface and the panel surface is considered as contact surface. Curvature of the surface, mesh size, stiffness of the surface, size of the surface, etc. decide which surface should be contact surface and which one be target surface.

There are many contact algorithms [40] like penalty method, augmented Lagrangian, Lagrange multiplier, multipoint constraint (MPC) out of which augmented Lagrangian method is employed here. It is the iterative series of penalty methods. It is less sensitive to the contact stiffness mag-

(a)   (b)

(c)   (d)
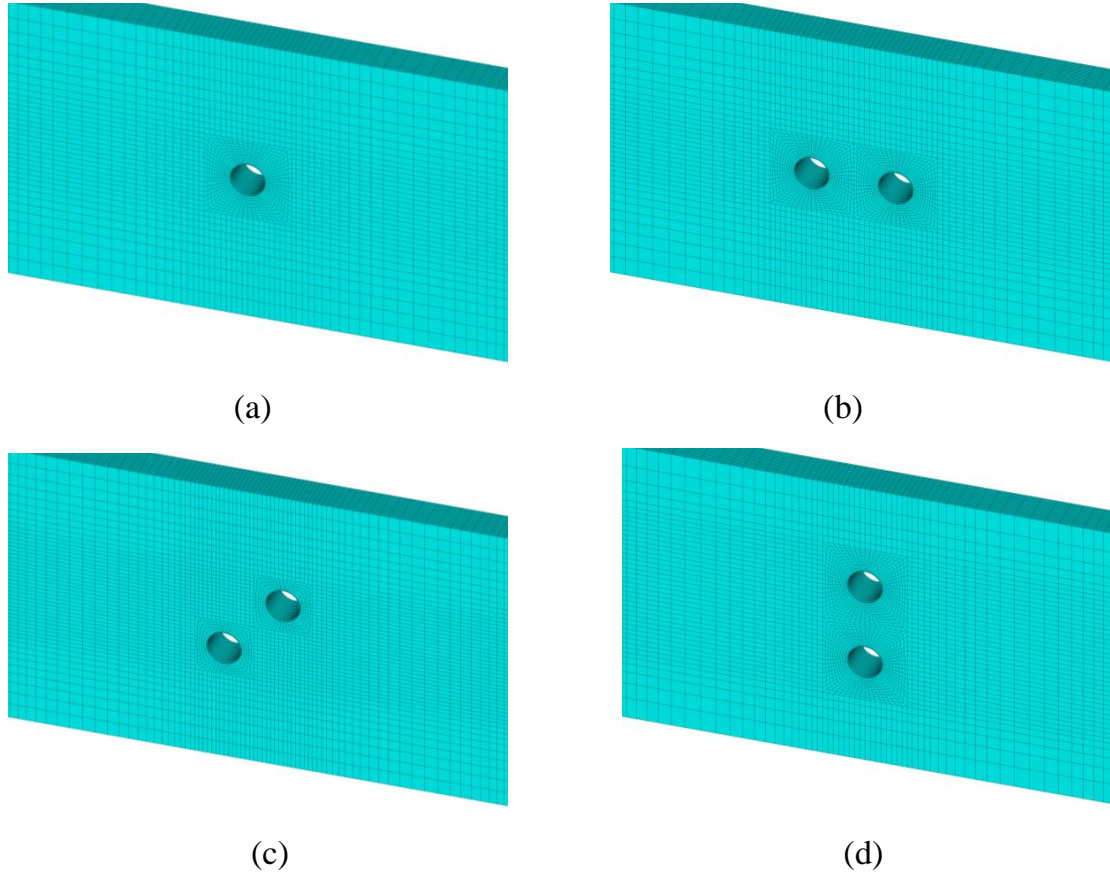
Figure 4.2: FEA models for panels having different hole configuration: (a) 1H, (b) 2HL, (c) 2HD and (d) 2HT

Table 4.1: Parameters chosen for contact elements

Parameters	Values
Initial penetration	Excluded
Contact adjustment	Closed gap initially
Contact algorithm	Augmented Lagrangian Method
Normal penalty stiffness factor	0.01
Penetration tolerance factor	0.2
Pinball region factor	1.0
Stiffness update	Each iteration

nitude. The equilibrium iterations keep going until the final penetration comes under the required tolerance during which the contact tractions are augmented. There are several contact parameters required to define the contact pair such as normal stiffness, tangential stiffness, penetration tolerance, friction coefficient, initial adjustment, pinball region, etc. These parameters dictates the convergence. The solution will not converge if inaccurate or inappropriate parameters are given. For augmented Lagrangian method, normal and contact stiffness have to be defined. Generally it needs to give a factor which calculates both stiffness values from material properties, element size, penetration tolerance, etc. The normal contact stiffness defines the amount of penetration and tan-

gential stiffness defines the amount of slip between the contact pairs. Tangential stiffness value is determined by the normal stiffness value and the friction coefficient. Higher stiffness value leads to convergence problems and lower stiffness value leads to more penetration and inaccurate solution. The penetration tolerance is affected by the depth of the underlying elements. If penetration is found out to be higher than the given tolerance value than the solution is considered as unconverged one and iterations keep going on to fall the penetration value under the mentioned tolerance value. In the contact analysis, initial penetration is excluded and closed the initial gap if any. Pinball region is selected carefully to avoid the contact detection problems. Its value defines the area into which it searches for target and contact elements. Its high value includes more contact elements but the computing process will be slowed down marginally.

4.4   Introduction to PDM

As discussed earlier, composites have various damage failures mainly called interlaminar and intralminar failures. Interlaminar failures includes delamination whereas intralminar failures include matrix cracking, fiber splitting, fiber kinking, fiber-matrix shear failure, etc. These all are interacting with each other. In progressive damage modelling (PDM) these all failures are considered for damage evolution. Damage initiation, damage propagation and ultimate failure load are observed through PDM and can be compared with experimental results. Once it is validated for majority of loading conditions, it can extended for failure prediction to the loading conditions where performing experiments is quite a challenging problem. PDM can be divided into three major steps: Stress analysis, damage predictions and damage modelling respectively. After the stress analysis through standard FEA software, damage is predicted by various failure criteria which gives a non-dimensional failure index for each element. If elements fail, damage is induced in those elements by degrading the material properties in a certain way. There are many methods available for degrading materials like material property degradation method (MPDM), continuum damage mechanics (CDM) method, etc. In MPDM, the material stiffness is instantly reduced according to the type of damage occurred and determined by physical failure criteria. In CDM, damage will not introduced instantly but gradually according to energy dissipated for the various damage modes. In this study, MPDM is implemented for the damage modelling. According to the mode of the damage, only selective material properties will be degraded to the 5% of the original one [41]. The flowchart of PDM algorithm is shown in fig. 4.3.

4.5   PDM involving Hashin's and Ye's delamination criterion

4.5.1   Introduction

In the present study, Hashin's failure criteria along with Ye's delamination criteria are used for PDM. It includes four modes of failures which are tensile and compressive failures of matrix and fiber. The failure theory is based on phenomenological models and can be applied to unidirectional laminates. Therefore, the failure criteria is calculated for each layer individually. It is interactive failure criteria so it is calculated using more than one stress components. It is a quadratic interaction between stress invariants.
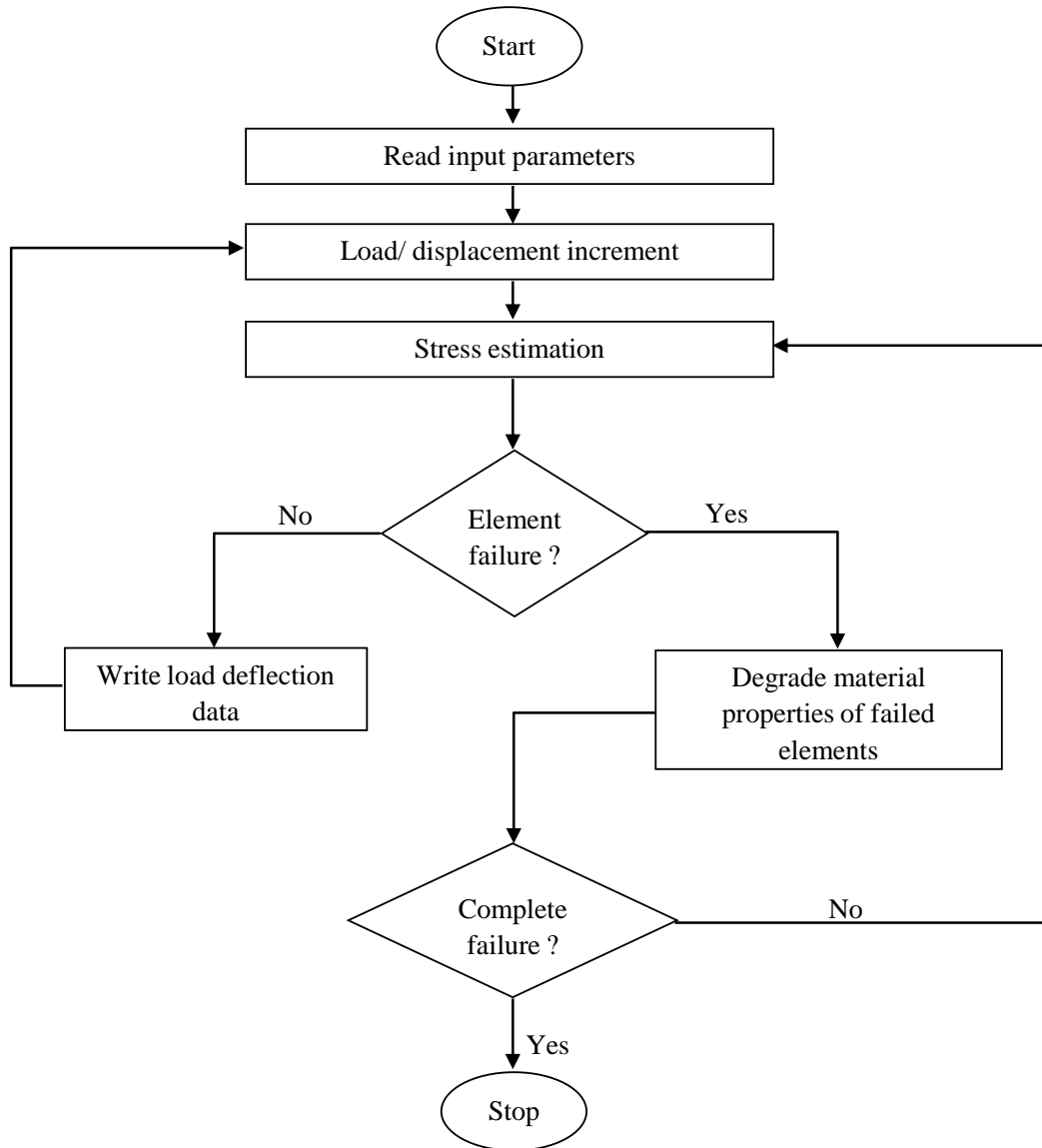
Figure 4.3: Flowchart of PDM [2]

Hashin's four criteria are given below :

1. Tensile fiber failure for $\sigma_{xx} \geq 0$

$$\left(\frac{\sigma_{xx}}{X_T}\right)^2 + \frac{\sigma_{xy}^2 + \sigma_{xz}^2}{S_{xy}^2} = \begin{cases} \geq 1 & failure \\ < 1 & no failure \end{cases} \tag{4.1}$$

2. Compressive fiber failure for $\sigma_{xx} < 0$

$$\left(\frac{\sigma_{xx}}{X_C}\right)^2 = \begin{cases} \geq 1 & failure \\ < 1 & no failure \end{cases} \tag{4.2}$$

3. Tensile matrix failure for $\sigma_{yy} + \sigma_{zz} \geq 0$

$$\frac{(\sigma_{xx} + \sigma_{zz})^2}{Y_T^2} + \frac{\sigma_{yz}^2 - \sigma_{yy}\sigma_{zz}}{S_{yz}^2} + \frac{\sigma_{xy}^2 + \sigma_{xz}^2}{S_{xy}^2} = \begin{cases} \geq 1 & failure \\ < 1 & nofailure \end{cases} \qquad (4.3)$$

4. Compressive matrix failure for $\sigma_{yy} + \sigma_{zz} < 0$

$$\left[\left(\frac{Y_C}{2S_{yz}}\right)^2 - 1\right]\left(\frac{\sigma_{yy} + \sigma_{zz}}{Y_C}\right) + \frac{(\sigma_{xx} + \sigma_{zz})^2}{4S_{yz}^2} + \frac{\sigma_{yz}^2 - \sigma_{yy}\sigma_{zz}}{S_{yz}^2} + \frac{\sigma_{xy}^2 + \sigma_{xz}^2}{S_{xy}^2} = \begin{cases} \geq 1 & failure \\ < 1 & nofailure \end{cases}$$
$$(4.4)$$

Ye's delamination criteria is based on transverse stress state. It is defined on whether the transverse normal stress is tensile or compressive. They are given as follow :

1. Interlaminar tensile failure for $\sigma_{zz} \geq 0$

$$\left(\frac{\sigma_{zz}}{Z_T}\right)^2 + \left(\frac{\sigma_{yz}}{S_{yz}}\right)^2 + \left(\frac{\sigma_{xz}}{S_{xz}}\right)^2 = \begin{cases} \geq 1 & failure \\ < 1 & nofailure \end{cases} \qquad (4.5)$$

2. Interlaminar compression failure for $\sigma_{zz} < 0$

$$\left(\frac{\sigma_{zz}}{Z_C}\right)^2 + \left(\frac{\sigma_{yz}}{S_{yz}}\right)^2 + \left(\frac{\sigma_{xz}}{S_{xz}}\right)^2 = \begin{cases} \geq 1 & failure \\ < 1 & nofailure \end{cases} \qquad (4.6)$$

where, σ_{ij} denote the stress components and the tensile and compressive allowable strengths for lamina are denoted by subscripts T and C, respectively. X_T, Y_T, Z_T denote the allowable tensile strengths in three respective material directions. Similarly, X_C, Y_C, Z_C denote the allowable compressive strengths in three respective material directions. Further, S_{xy}, S_{yz}, S_{xz} denote allowable shear strengths in the respective principal material directions.

The material properties used for PDM are determined as per various ASTM standards. 3D-DIC system is used for material characterization [42]. The properties are given in Table 4.2.

Table 4.2: CFRP composite laminate properties

Properties	Values
Longitudinal modulus, E_{11} (GPa)	82.46
Transverse modulus, $E_{22} = E_{33}$ (GPa)	7.12
In-plane Shear modulus, $G_{12} = G_{13}$ (GPa)	3.30
Out-of-plane Shear modulus, G_{23} (GPa)	2.47
In-plane Poisson's ratio, $\nu_{12} = \nu_{13}$	0.31
Out-of-plane Poisson's ratio, ν_{23}	0.43
Longitudinal tensile strength, X_T (MPa)	1080
Longitudinal compressive strength, X_C (MPa)	600
Transverse tensile strength, Y_T (MPa)	35
Transverse compressive strength, Y_C (MPa)	90
In-plane shear strength, $S_{12} = S_{13}$ (MPa)	57
Out-of-plane shear strength, S_{23} (MPa)	28.5
Mode-I fracture toughness, G_{Ic} (kJ/mm^2)	1.05
Mode-II fracture toughness, G_{IIc} (kJ/mm^2)	1.25

4.5.2 Results and discussions

UD CFRP panels

Load-displacement curves predicted by PDM simulations for composite panels for 1H, 2HL, 2HD and 2HT configurations are compared with the corresponding experimental behaviour as shown in Fig. 4.4. It is observed that load-displacement behaviour obtained from PDM through Hashin's and Ye's delamination criteria underpredicts the load and displacement as well in case of 1H and 2HL. PDM predictions of ultimate load and corresponding displacement in case of CFRP panel having 2HD configuration agrees well with experimental results. For the panel with 2HT configuration, PDM predicts the ultimate load near to the experimental one but underpredicts the corresponding displacement.

(a) 1H   (b) 2HL

(c) 2HD   (d) 2HT
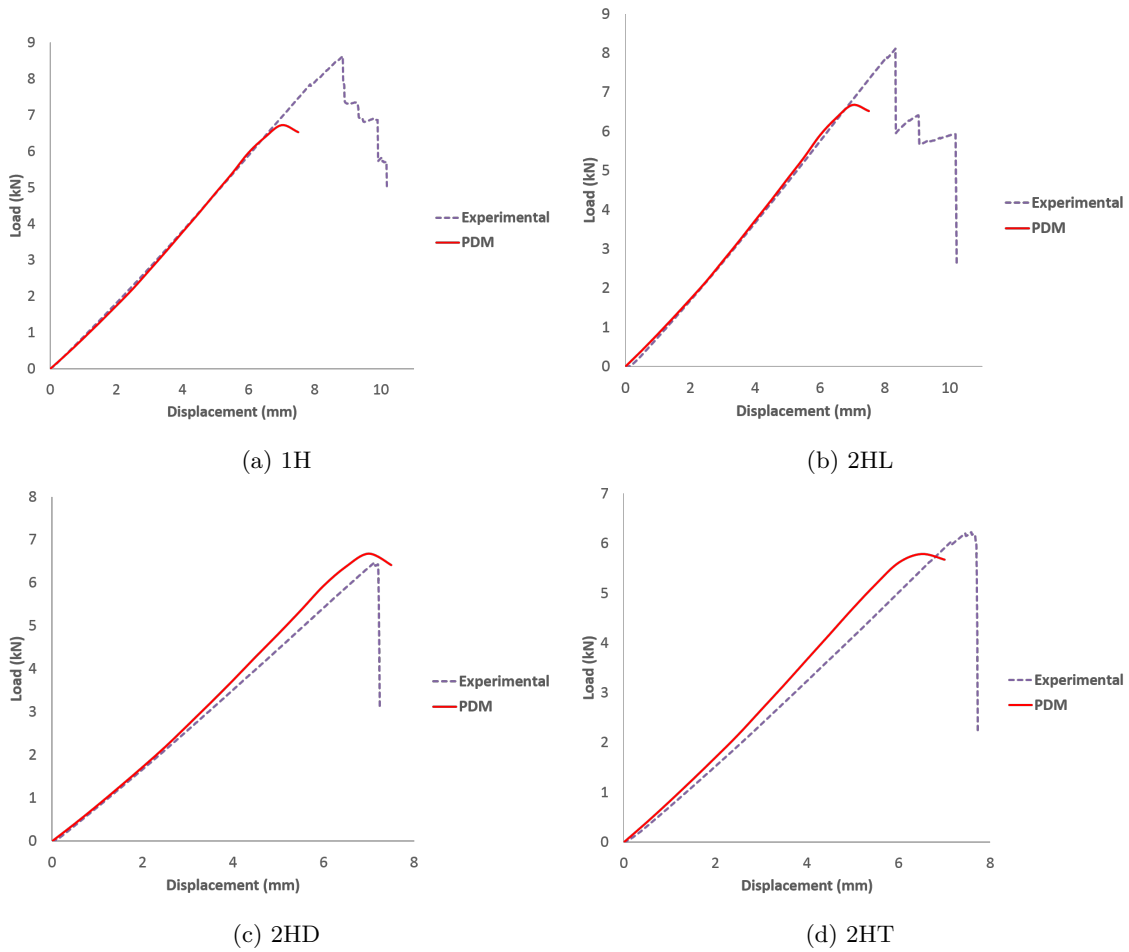
Figure 4.4: Load-displacement behaviour for UD CFRP panels with different hole configurations

These deviations of PDM predictions from experimental results may occurred due to the the choice and implementation of failure theory. It significantly affects the accuracy of the PDM prediction. It seems that Hashin's fiber and matrix tensile failure predicts the damage quite well. However, it underpredicts the matrix and fiber compressive failures. Several composite failure theories perform well in specific cases and poor in others, suggesting trial and error basis for selection. Besides this, prediction of PDM is also dependent on the rules of damage modelling. The material property

degradation rule and degradation factor can affect the results of PDM. The above mentioned reasons could cause underpredictions.

Among multiple hole configurations, 2HL is preferred since it has got higher in initiation and final failure load. Figs. 4.5 - 4.8 shows detailed illustrations of damage propagation predicted for plywise damage progression in UD CFRP panels for 1H, 2HL, 2HD and 2HT configurations respectively at different load levels. It is found out that damage initiation is detected first in the outermost ply on compression side because it comes under highest flexural stress and CFRP has low compressive strength. On compression side, the inner subsequent plies starts failing after some loadsteps later. However, the damage progression is found out to be the similar manner as that of outer-most ply in compression. Initially the damage on compression side starts propagating in longitudinal direction. Later, it drastically propagates in transverse direction from the hole. There is less amount of the damage found on tension side outer-most ply due to high tensile strength of CFRP panels. Damage is propagating in the longitudinal direction in all tension side plies as load increases.

Figure 4.5: Illustration of damage propagation predicted by the PDM with increasing load for UD CFRP laminate having 1H configuration

The ultimate failure load and corresponding displacement are tabulated in Table 4.3. It is observed that composite panel with 2HL configuration sustain highest load compared to other two multiple hole configuration. It is observed that a significant amount of damage is accumulated around the holes. In all the plies, damage starts with either matrix compression or matrix tensile failure. Damage initiates near the hole and propagates in longitudinal direction. Though Ye's delamination criteria is implemented, no significant delamination is found out in case of UD CFRP panels.

Figure 4.6: Illustration of damage propagation predicted by the PDM with increasing load for UD CFRP laminate having 2HL configuration

Figure 4.7: Illustration of damage propagation predicted by the PDM with increasing load for UD CFRP laminate having 2HD configuration
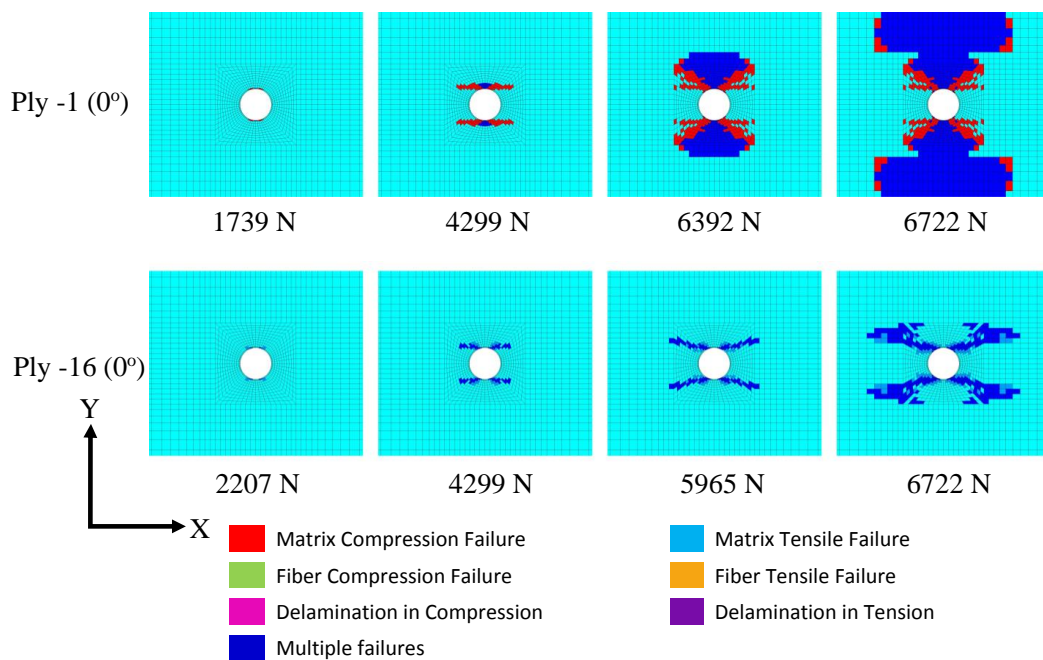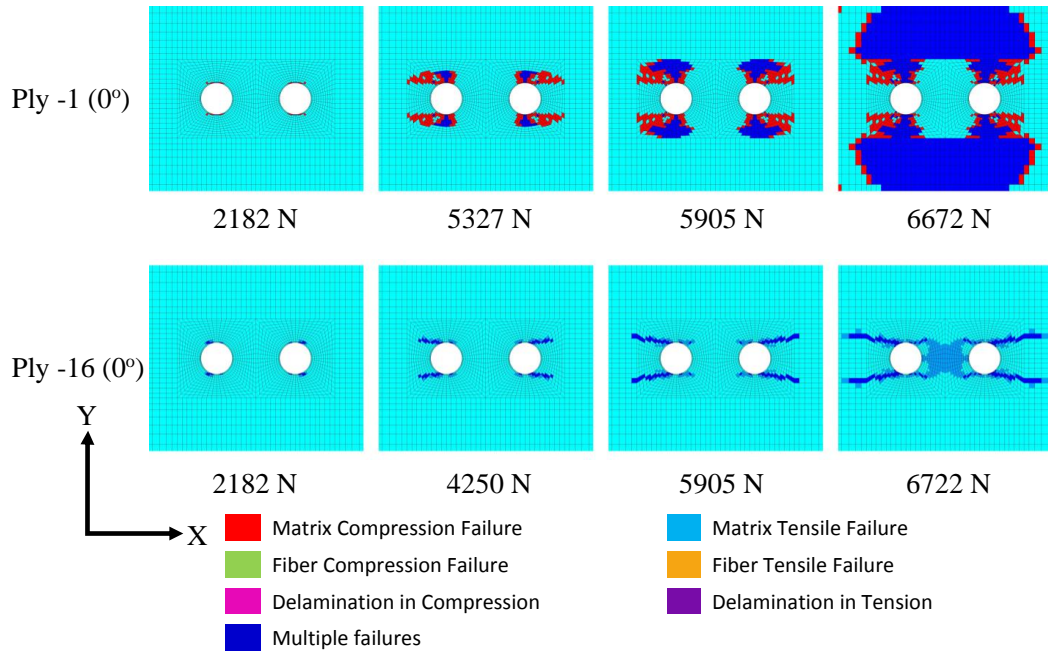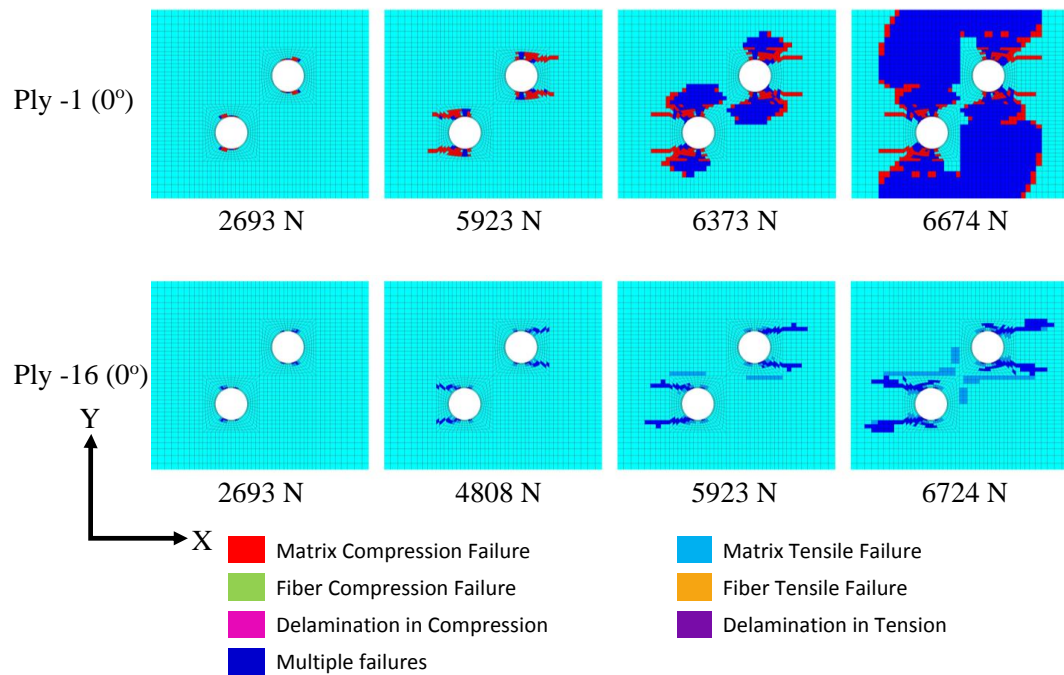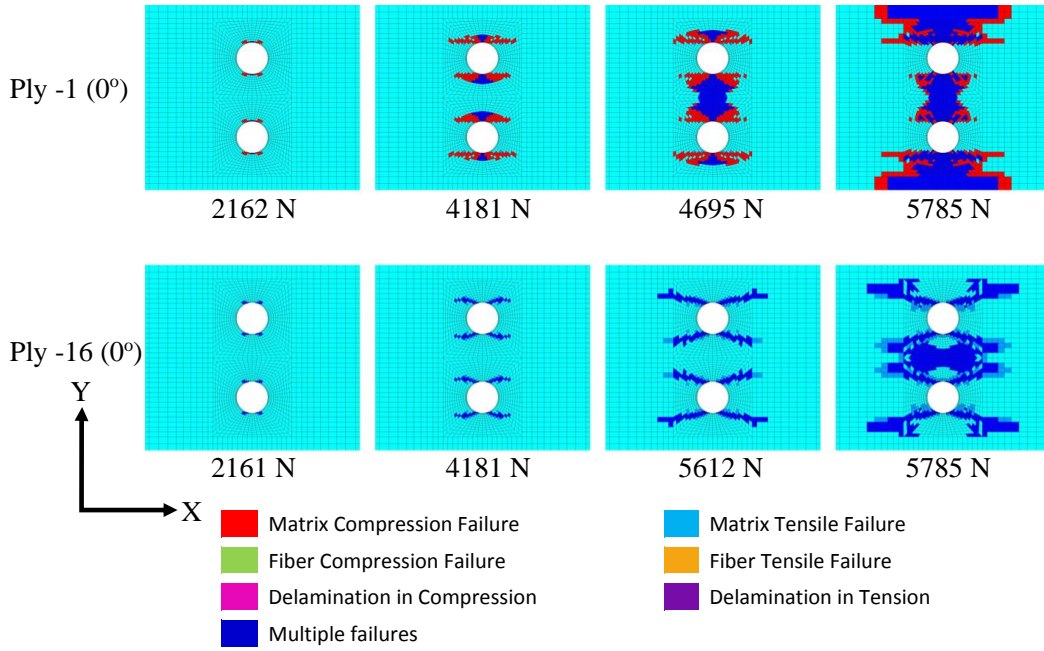
Figure 4.8: Illustration of damage propagation predicted by the PDM with increasing load for UD CFRP laminate having 2HT configuration

Quasi CFRP panels

The quasi CFRP panels with layup sequence $[+45/0/-45/90]_{2S}$ is analysed under flexural loading with different single and multiple hole configurations. The relative comparison between experimental and PDM predicted load-displacement is shown in Fig. 4.9. Ultimate load and corresponding displacement are tabulated in Table 4.4 Underprediction of the ultimate load and corresponding displacement is also found out here in case of quasi CFRP panels. The load carrying capacity of quasi panels are found out to be less in each configurations of CFRP panels than those of UD panels. However, due to distributed fiber orientation in all directions, panels become more compliant and have more displacements corresponding to the final failure compared to UD panels. When a ply is constrained through the plies having different fiber orientation, it has a slight increase in the strength than the that of unconstrained ply. This effect should be considered while analysing the quasi CFRP panels. In this study, Hashin's criteria is implemented without this correction of strength. Ye's criteria is included in the PDM for delamination. However, failure should occur on both side of the interface when delamination occurs. Ye's delamination criteria is only predicting the delamination on one side. This limitation can affect the overall PDM results and cause the underprediction.

The damage propagation with increasing flexural load for CFRP panels with different hole configurations is shown in Figs. 4.10 - 4.17. In all the cases, damage initiates in the outer-most ply with 45° fiber orientation on compression side. It initiates in the transverse direction near the holes in form of matrix compression failure. It is observed that there is no significant fiber breakages found on the outer-most ply. The ply underneath it has 0° fiber orientation. The load carrying capacity of
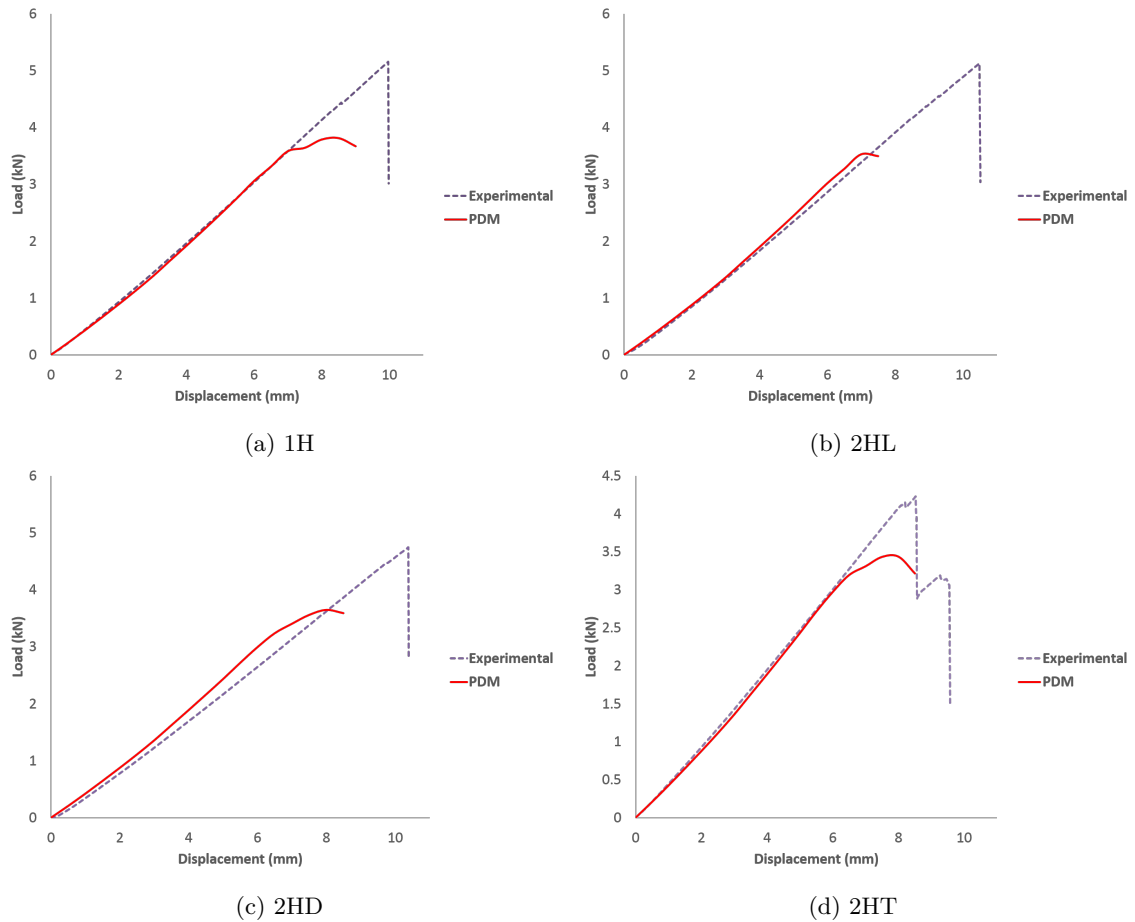
Figure 4.9: Load-displacement behaviour for quasi CFRP panels with different hole configurations

the panel is mostly dependent on this ply because it is the outer-most $0°$ ply which takes more load than any other ply. The fiber breakages (compression failure) can be found on this layer. The panel will fail once this ply fails. The subsequent ply with $-45°$ fiber orientation has damage initiation at higher loads because of lower distance from the neutral axis. Damage propagates in the transverse direction in form of matrix compression failure. The damage in fourth ply with $90°$ fiber direction is found out to be very less and it propagates in $-45°$ direction. Delamination can be observed in this ply with matrix tensile failure.

In the tension side, damage initiates and propagates in the transverse direction for all the plies. All plies except $0°$ ply fails mainly due to matrix tensile failure. The fifteenth ply having $0°$ fiber orientation fails additionally due to fiber tensile failure. There is no delamination observed in any plies on the tension side.

Delamination in case of quasi CFRP panels is severe but Ye's failure criteria is not able to detect this failure accurately. There is a need to model the delamination failure through other means so that it can be captured accurately. One way to model delamination failure is cohesive zone modelling (CZM).

33

Figure 4.10: Illustration of damage propagation of first four plies (compression side) predicted by the PDM with increasing load for quasi CFRP laminate having 1H configuration

Ply-13 (90°)

1376 N   3582 N   3641 N   3787 N

Ply-14 (-45°)

1647 N   3641 N   3787 N   3810 N

Ply-15 (0°)

1916 N   3641 N   3787 N   3810 N

Ply-16 (45°)

1376 N   3312 N   3060 N   3641 N

Matrix Compression Failure   Matrix Tensile Failure
Fiber Compression Failure   Fiber Tensile Failure
Delamination in Compression   Delamination in Tension
Multiple failures

Figure 4.11: Illustration of damage propagation of last four plies (tension side) predicted by the PDM with increasing load for quasi CFRP laminate having 1H configuration

35

Figure 4.12: Illustration of damage propagation of first four plies (compression side) predicted by the PDM with increasing load for quasi CFRP laminate having 2HL configuration

Figure 4.13: Illustration of damage propagation of last four plies (tension side) predicted by the PDM with increasing load for quasi CFRP laminate having 2HL configuration

Figure 4.14: Illustration of damage propagation of first four plies (compression side) predicted by the PDM with increasing load for quasi CFRP laminate having 2HD configuration

Figure 4.15: Illustration of damage propagation of last four plies (tension side) predicted by the PDM with increasing load for quasi CFRP laminate having 2HD configuration
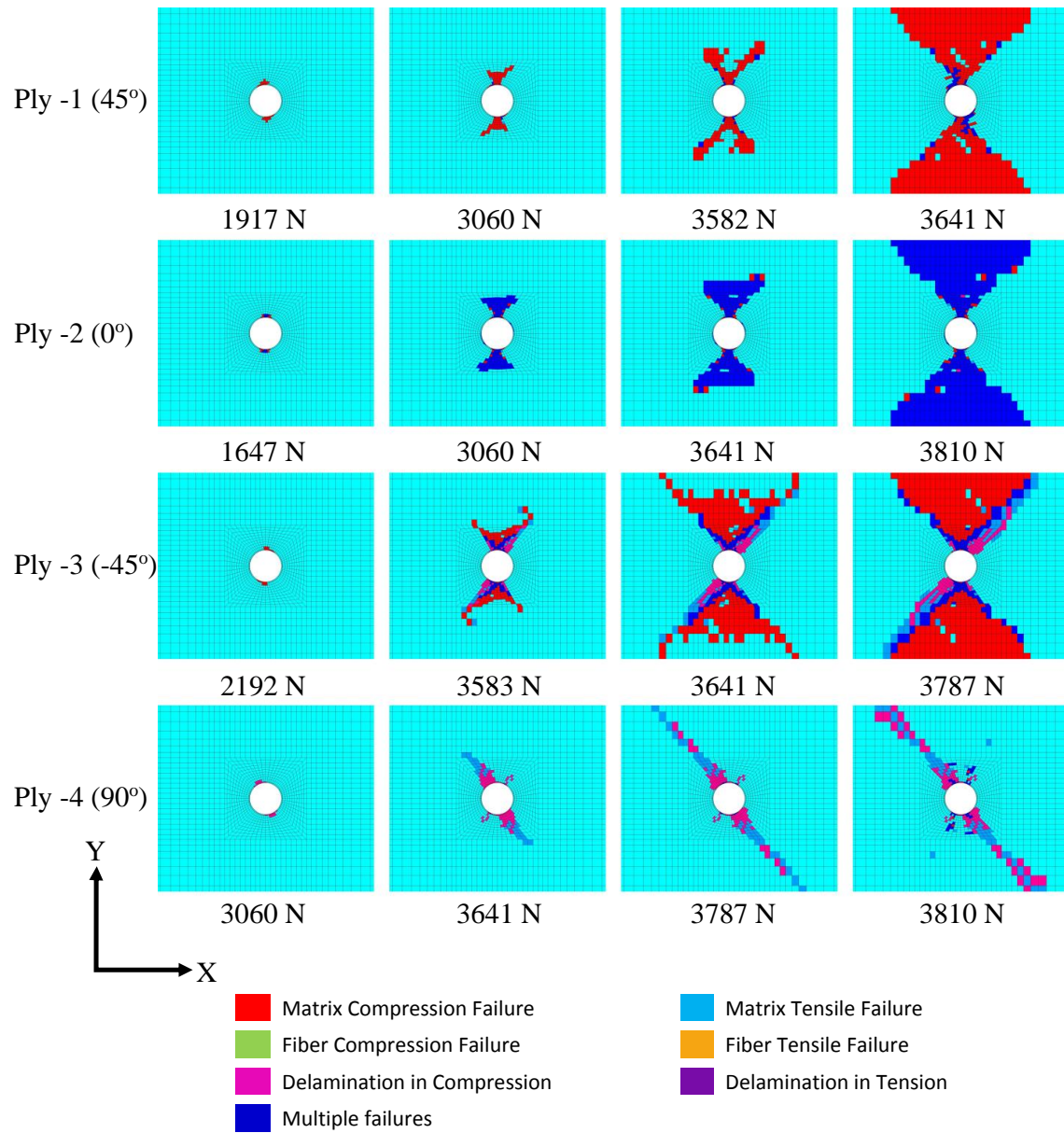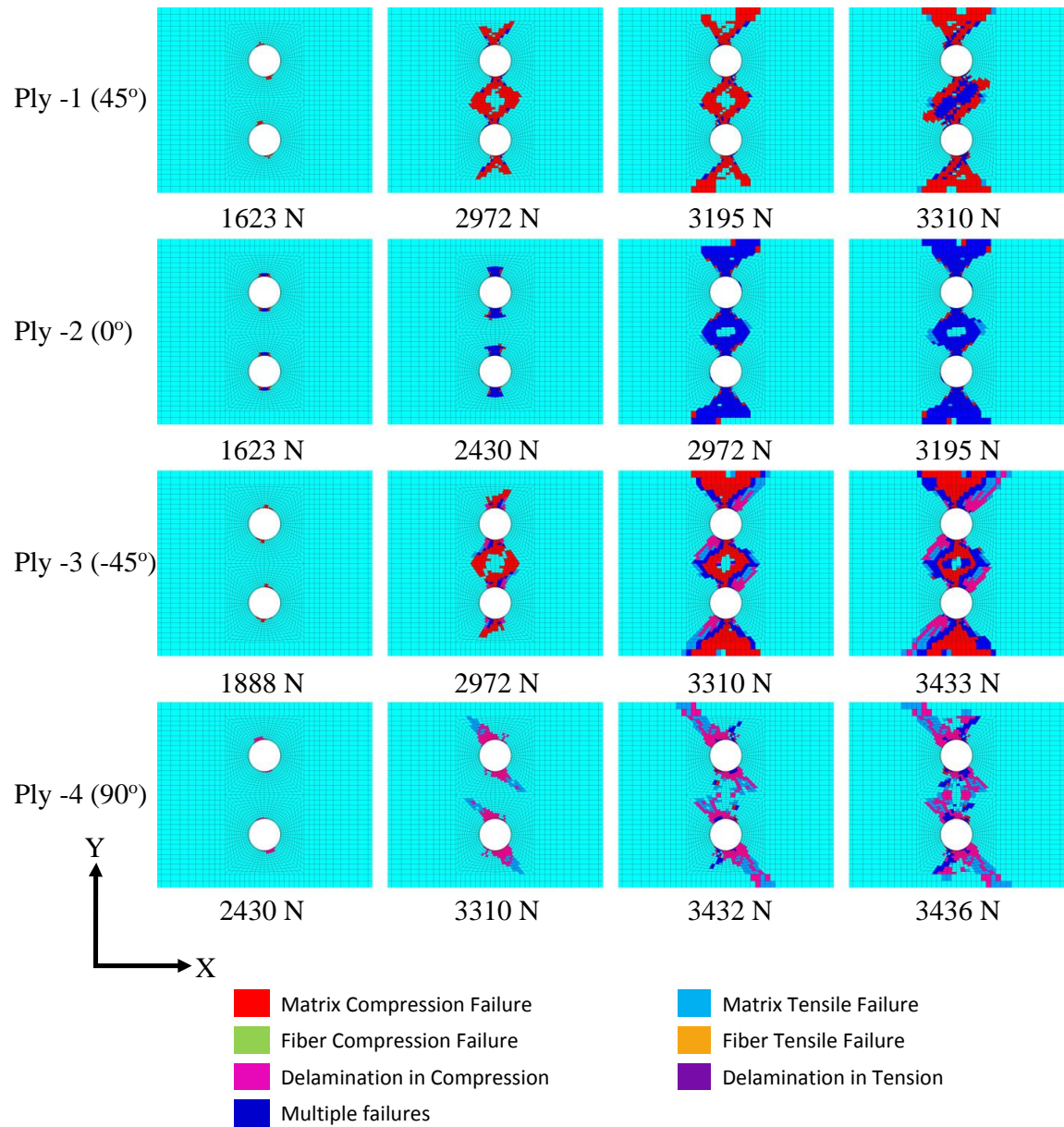
Figure 4.16: Illustration of damage propagation of first four plies (compression side) predicted by the PDM with increasing load for quasi CFRP laminate having 2HT configuration
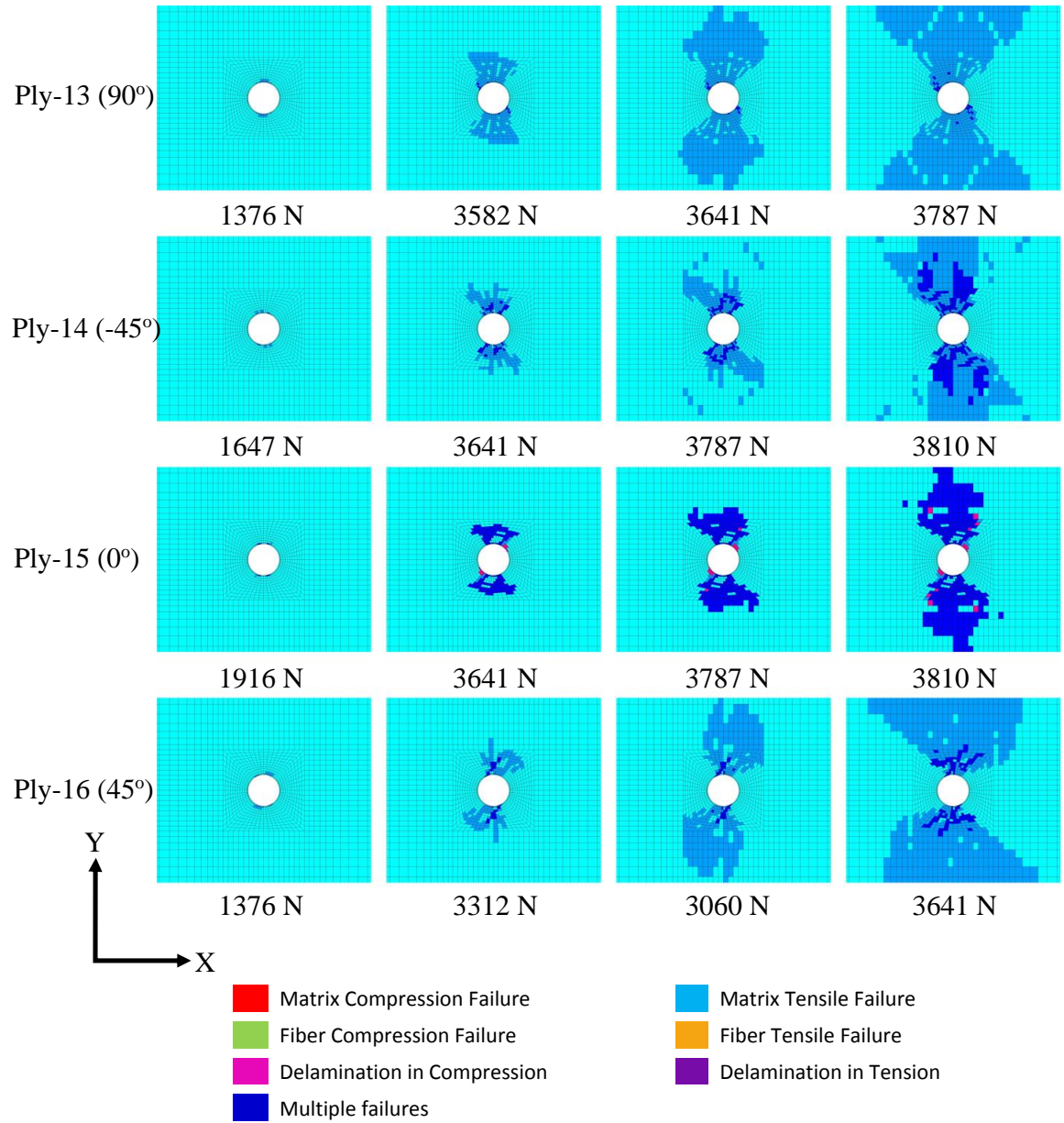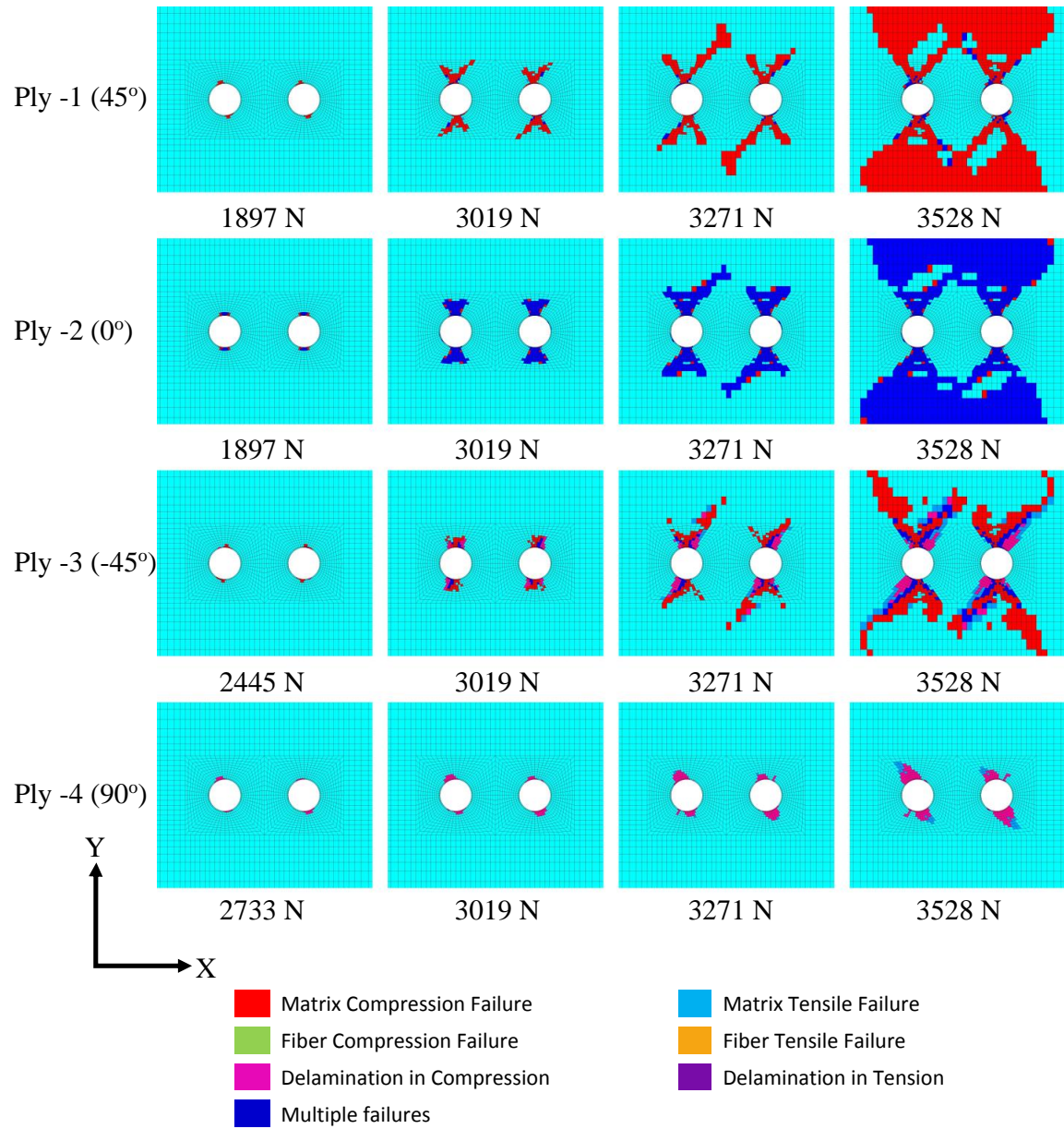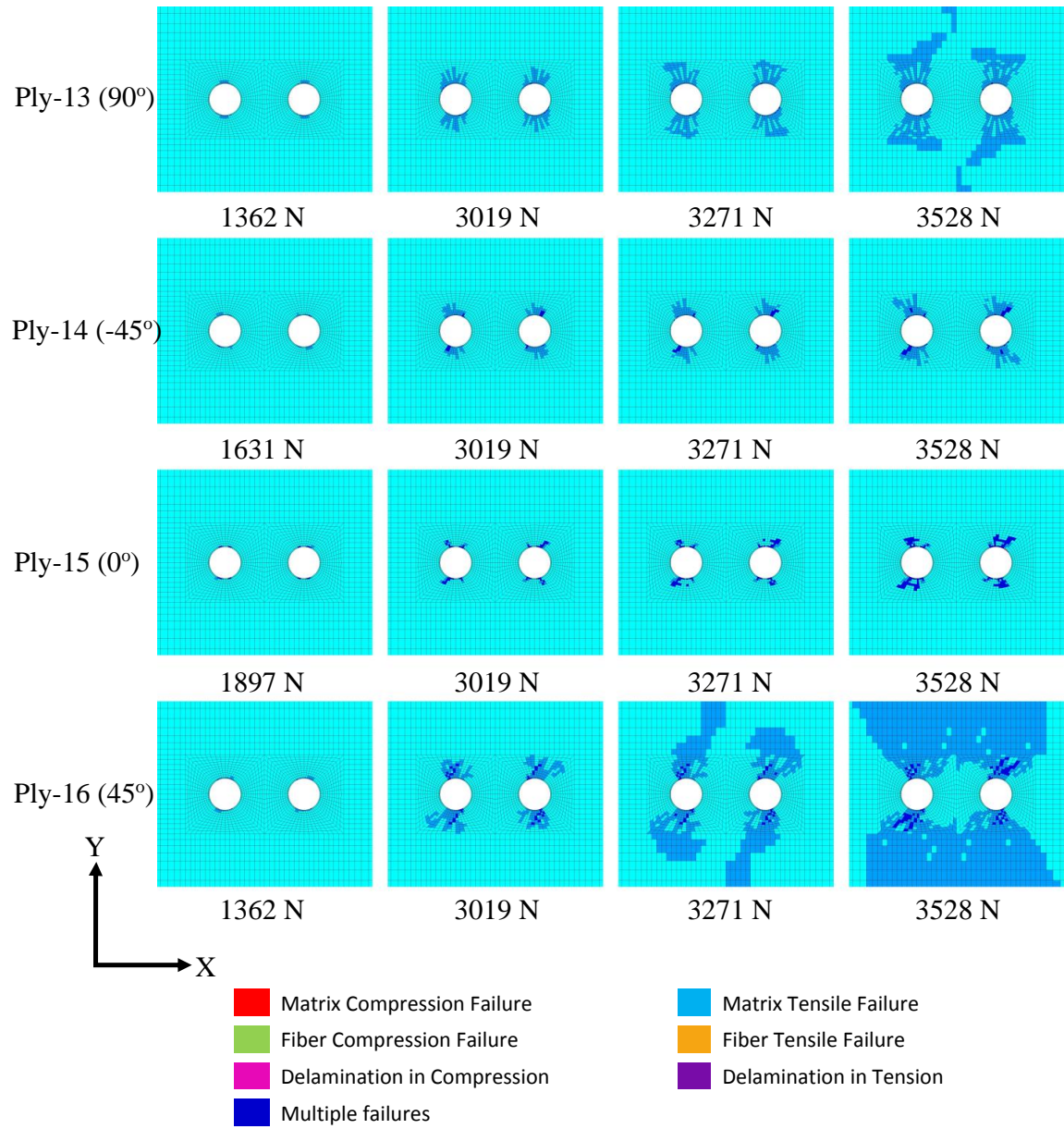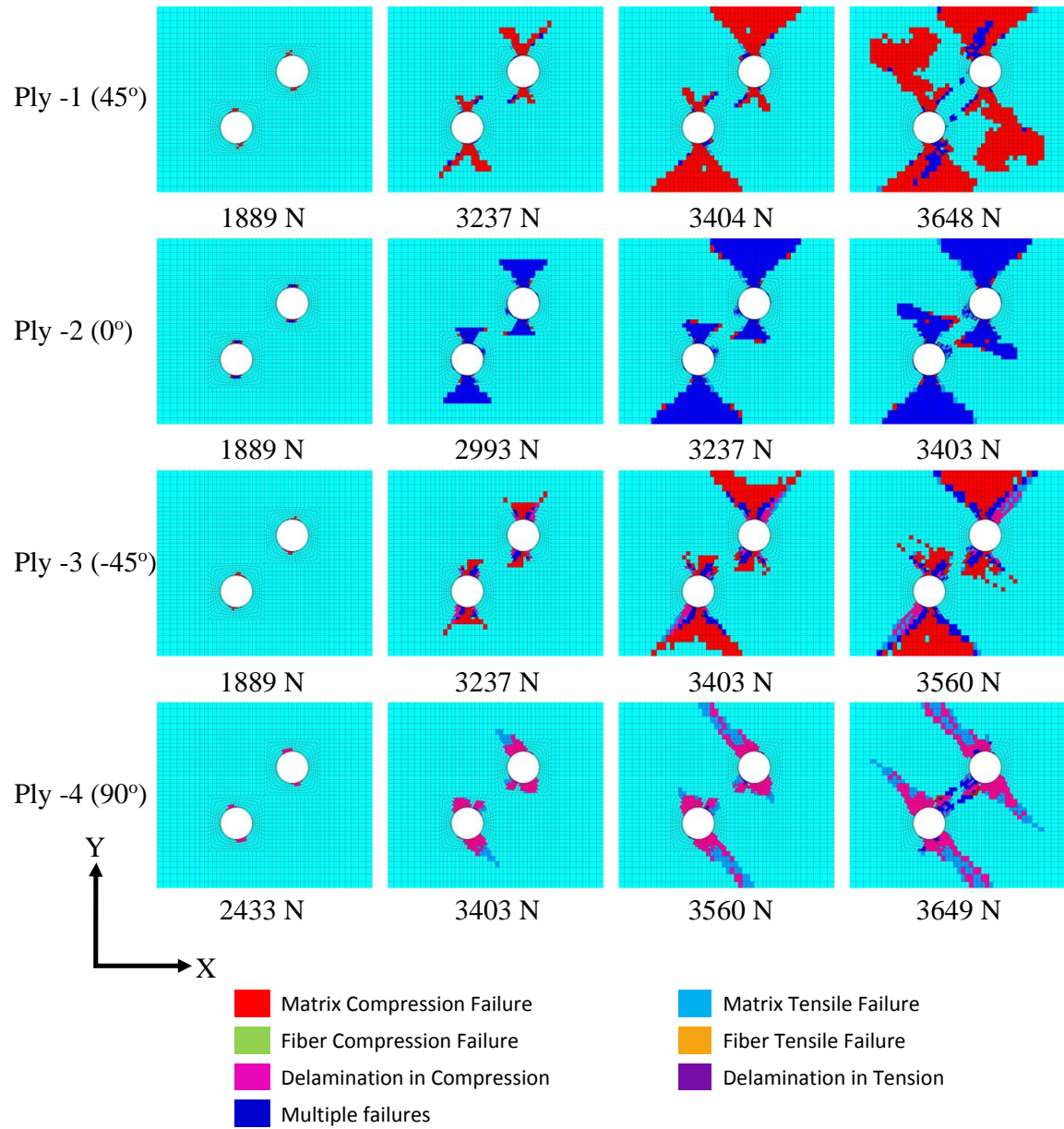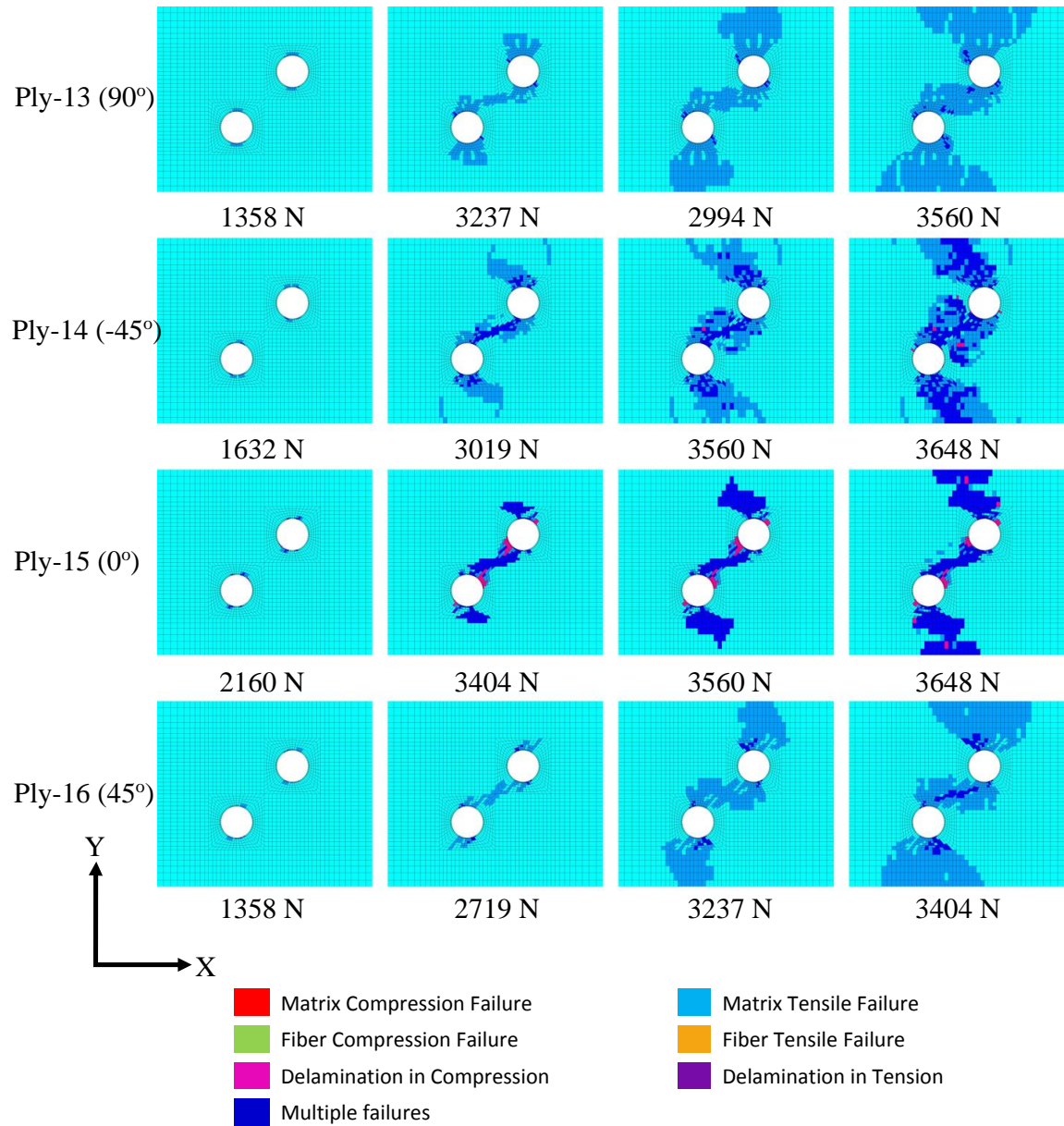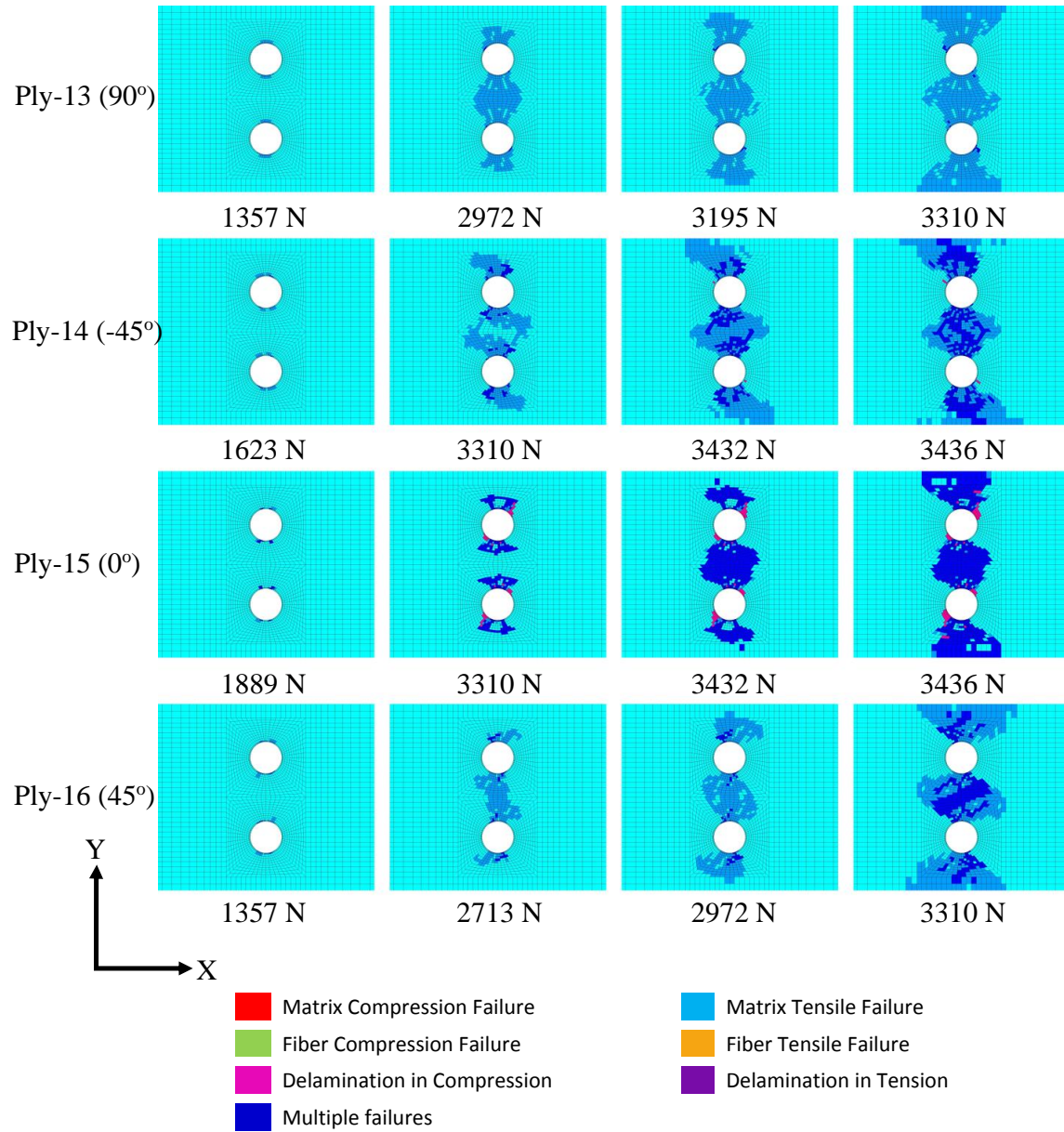
Figure 4.17: Illustration of damage propagation of last four plies (tension side) predicted by the PDM with increasing load for quasi CFRP laminate having 2HT configuration

4.6 Delamination modelling and growth through CZM

4.6.1 Introduction

Delamination between the layers in layered composites is vary critical and reduces the stiffness and toughness of the composite structures marginally. Interface delamination can be modelled through fracture mechanics by employing softening relationships between tractions and separations.Therefore if there is more energy available than critical fracture energy, delamination will start to propagate. This is the basic concept of cohesive zone modelling (CZM). There are many traction-separation laws for CZM like exponential behaviour, bilinear behaviour, trapezoidal, etc. Among these, exponential law is the coupled mixed mode law [33] whereas other mentioned can be modelled with individual mode-I and mode-II separation as shown in fig. 4.18. In this study, bilinear behaviour is considered for the CZM. It can be modelled with pure mode-I, pure mode-II or mixed mode loading. To define the bilinear law, it is required to get the values maximum traction, initial stiffness and the separation at the completion of debonding or delamination. One of the major problem regarding CZM is the mesh dependency and convergence issues with coarser mesh. Therefore it is a major challenge while determining constitutive parameters for CZM.
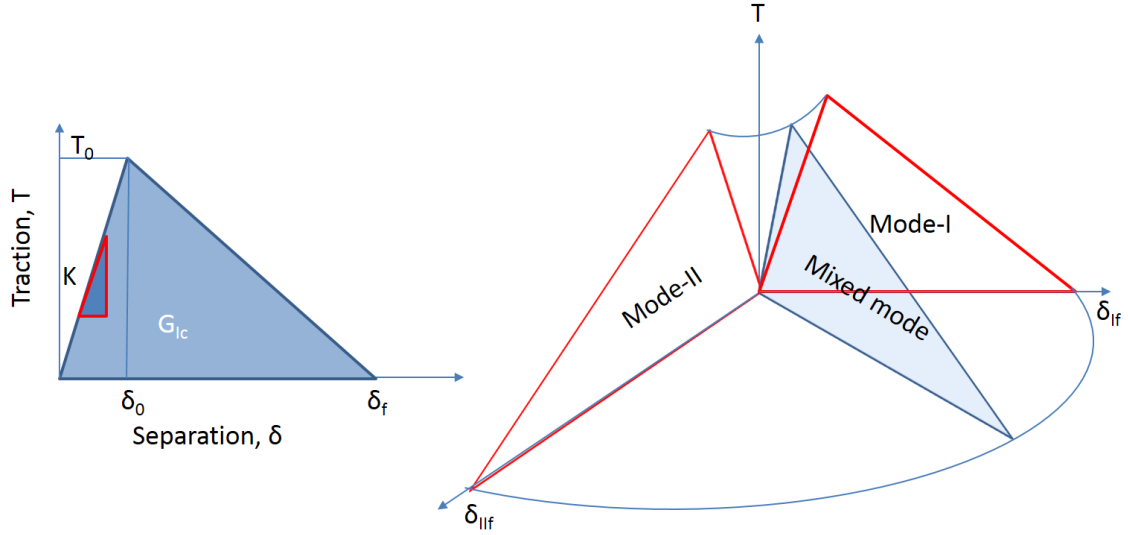
Figure 4.18: Traction-separation law for CZM

4.6.2 Calibration of CZM properties

Turon el al. [34] have established a procedure to determine the optimal CZM parameters for delamination. The initial stiffness of the bilinear law is defined through thickness of the laminate (t), transverse Young's modulus (E_3) and a scalar parameter (α) to control the overall stiffness in transverse direction. Generally the value of the initial stiffness should be very high so that it cannot affect the effective ealstic properties of the composites.

$$K = \frac{\alpha E_3}{t} \tag{4.7}$$

After defining the initial stiffness, the separation can be calculated if the interfacial strength of the composite is known. The area under the curve of traction-separation law is equivalent to mode-I and mode-II fracture toughness. Therefore, the separation at the completion of the delamination can also calculated from fracture toughness and interfacial strength. To get the accurate delamination prediction, there should be enough number of elements in the cohesive zone. The length of the cohezive zone is defined as :

$$l_{cz} = ME_3 \frac{G_c}{(T^0)^2} \tag{4.8}$$

where,

E_3 = Transverse Young's modulus

M = Parameter as per cohesive zone model

G_c = Fracture toughness

T^0 = Maximum inter-facial strength

The length of cohesive zone for CFRP composite comes out to be 3.17 mm. It is good practice to include at least five elements in the cohesive zone. The length of the CZM element in the direction of delamination propagation is suggested to be 0.634 mm. However, the length of the element is kept 0.5 mm, below than the suggested one. DCB and ENF specimen have width of 25 mm. Therefore, they are modelled with PLANE183 elements (plain strain condition) along with INTER193 interface element for CZM. DCB is modelled with 3000 PLANE183 and 150 interface elements. The analysis is carried out in displacement control. One end of DCB is completely constrained while at the other end,opposite displacement in vertical direction is given to each hand of delaminated part. ENF is modelled with 3960 plane elements along with 220 interface elements. The contact pair is created between upper initially delaminated part with the lower one in case of ENF. Friction co-efficient is to be chosen 0.25. Same contact parameters for the contact pair are applied here also listed in Table 4.1. Three-point bending is applied to the model. The span length is kept 100 mm and load is applied at 50 mm away from one of the supporting node. The reaction force coming out from the analysis is integrated across the width to get the total reaction force. The load-displacement curves of FEM results are compared with the experimental one.

One parametric study is carried out to know the effect of change the shape of bilinear law. Therefore, the maximum traction is changed keeping maximum separation constant and vice versa. It is found that the shape of the traction-separation law does not affect the macromechanical behaviour (load-displacement profile) unless and until the area under the curve i.e. fracture toughness is changed (see fig. 4.19). The delamination propagation and stress distribution near the delamination front may get changed.

It is observed that there are convergence issues in CZM analysis for both the models. It can be overcome by introducing the artificial damping into CZM modelling to stabilize the delamination propagation [43]. By introducing the viscous regularization the convergence issues are removed and there is no any significant change in the load-displacement profile as can be seen in fig. 4.20 and fig. 4.21.
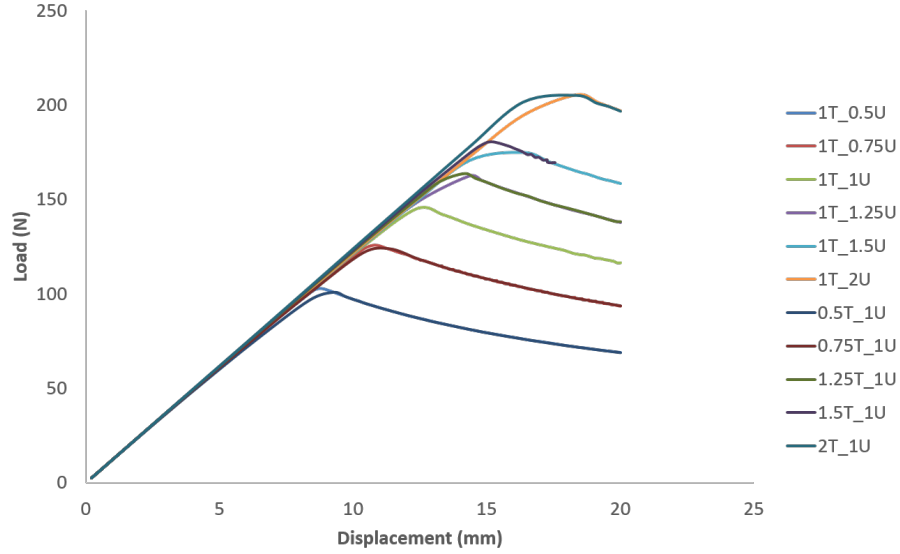
Figure 4.19: Load-displacement curves for various traction and separation parameters
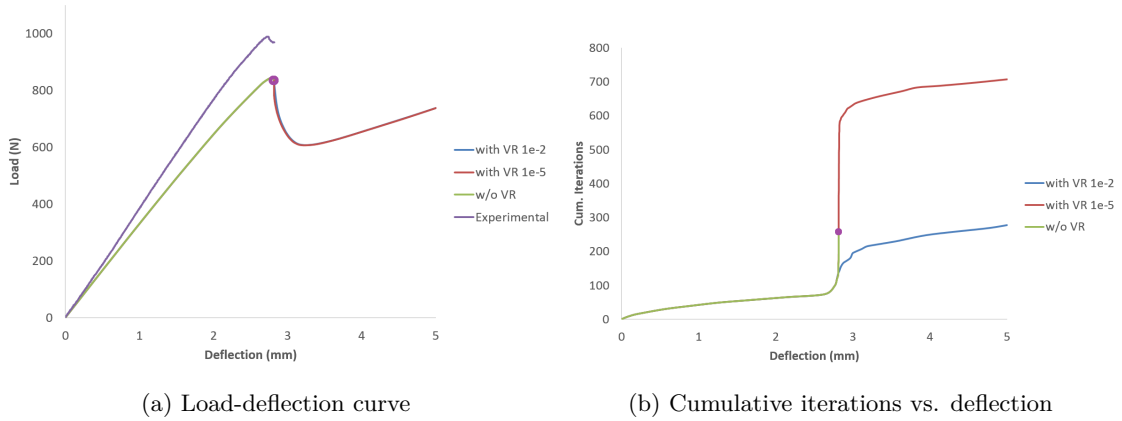
(a) Load-deflection curve

(b) Cumulative iterations vs. deflection

Figure 4.20: Viscous regularization in case of ENF

4.7 LaRC04 criteria

4.7.1 Introduction

The difficulty in the PDM development is to correlate the failures which occurs at microlevel and the material response at macro or meso level. As discussed above, Hashin's failure criteria is solely phenomenal based theory. There is no connection between the physics behind the failure and its material response. It is just quadratic fit of stress invariants with the experimental results. It is observed from the PDM results (discussed in Sec. 4.5.2) that Hashin's failure criteria under-predicts the fiber and matrix compression failures. That leads to very low load carrying capacity because it aids to the weakness of composite in compression. Therefore, there is need to develop PDM with more accurate and physics based failure criteria like Puck's , LaRC04, etc. In this study, LaRC04 [28] is used for this purpose. It consists basically of four damage modes which are matrix and fiber tensile and compressive failure. It includes the in-situ effects of the thickness and fiber orientation

44

(a) Load-deflection curve   (b) Cumulative iterations vs. deflection
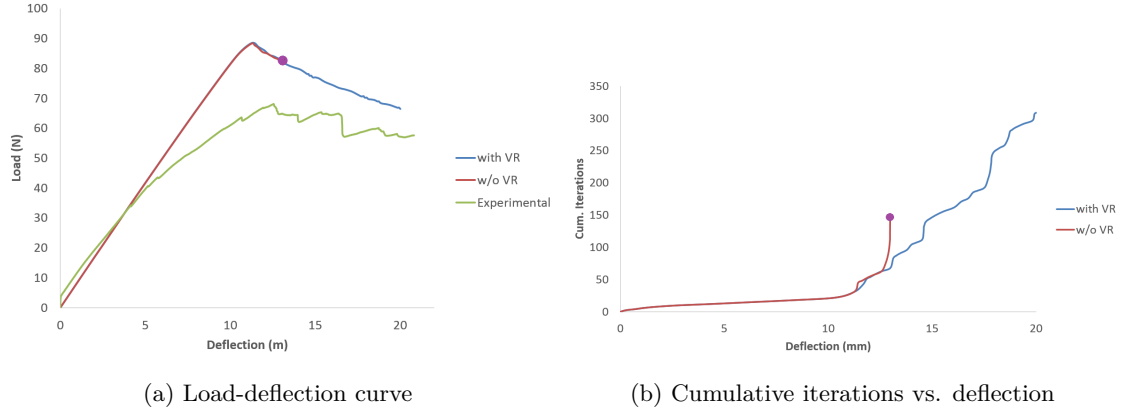
Figure 4.21: Viscous regularization on case of DCB

on the strength of the ply. Also, the non-linear shear behaviour of the composite is considered in the formulation. The fiber tensile failure is kept as simple as the ratio of longitudinal stress and the corresponding tensile strength. Two types of damages is considered for fiber compressive failure. First one is Fiber kinking and other one is the subsequent failure of the fibers due to matrix failure in transverse tension. In the matrix compressive failure, the friction effect in considered through Mohr-Coulomb failure theory. The matrix tensile failure is formulated from matrix cracking due to transverse tension. It is based on fracture mechanics arrived through Eshelby's inclusion problem.

4.7.2 Effect of thickness and fiber orientation on the strength of the ply

It is observed that the strength of the ply increases when it is constrained by the plies having different fiber orientation. Also thick plies have can have high density of matrix cracking. To includes these two effects, strengths determined from the experimental characterization have to be modified. For thick plies having thickness more than 0.7 mm, The transverse tensile (Y_T) and longitudinal shear (S^L) strengths are modified as follow:

$$Y_{is}^T = 1.12\sqrt{2}Y_T \tag{4.9}$$

$$S_{is}^L = \sqrt{2}S^L \tag{4.10}$$

For thin plies the same are modified as :

$$Y_{is}^T = \sqrt{\frac{8G_{Ic}}{\pi t \Lambda_{22}^0}} \tag{4.11}$$

where,

$$\Lambda_{22}^0 = 2\left(\frac{1}{E_{22}} - \frac{\nu_{21}^2}{E_{11}}\right) \tag{4.12}$$

$$S_{is}^L = \sqrt{\frac{8G_{12}G_{IIc}}{\pi t}} \tag{4.13}$$

It is to be noted that these modifications are purely based on fracture mechanics and only have

to be applied when the ply is constrained with ply having different fiber orientation.

4.7.3 Mohr-Coulomb criteria

Generally matrix material in compression fails due to shear. Therefore, the fracture angle should be $45°$ along the maximum shear stress plane ideally but the experimental results indicate the fracture angle to be $53\pm2°$ for most composite material because of the friction effect. Mohr-Coulomb criteria is considering this friction stress as an increment in shear strength. Matrix fails due to transverse loading and this criteria is helpful to get the compressive failure based on physical model. First of
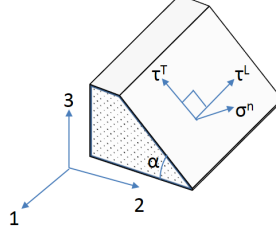
Figure 4.22: Stress transformation on fracture plane

all, tractions are derived for the fracture plane having plane angle α,

$$\begin{cases} \sigma_n = \frac{\sigma_{22}+\sigma_{33}}{2} + \frac{\sigma_{22}-\sigma_{33}}{2}cos(2\alpha) + \tau_{23}sin(2\alpha) \\ \tau^T = -\frac{\sigma_{22}-\sigma_{33}}{2}sin(2\alpha) + \tau_{23}cos(2\alpha) \\ \tau^L = \tau_{12}cos(\alpha) + \tau_{31}sin(\alpha) \end{cases} \tag{4.14}$$

M-C failure criteria can be now defined as:

$$\mid \tau^T \mid +\eta^T \sigma_n = S^T \tag{4.15}$$

Transverse friction coefficient η^T and transverse shear strength S^T from transverse compression strength S^T and fracture angle α_0 can be calculated as:

$$\eta^T = -\frac{1}{tan(2\alpha_0)} \tag{4.16}$$

$$S^T = Y^C cos(\alpha_0)\left(sin(\alpha_0) + \frac{cos(\alpha_0)}{tan(2\alpha_0)}\right) \tag{4.17}$$

Longitudinal friction coefficient is calculated as:

$$\frac{\eta^L}{S^L} = \frac{\eta^T}{S^T} \tag{4.18}$$

4.7.4 Fiber kinking

Fiber kinking is localized shear failure of the matrix along a band and subsequent fiber breakage near the edges of the band. In 3D kinking model, the possibility of the kinking will be in the principal

plane oriented at an angle ψ (see fig. 4.23)that can be calculated as:

$$tan(2\psi) = \frac{2\tau_{23}}{\sigma_{22} - \sigma_{33}} \qquad (4.19)$$
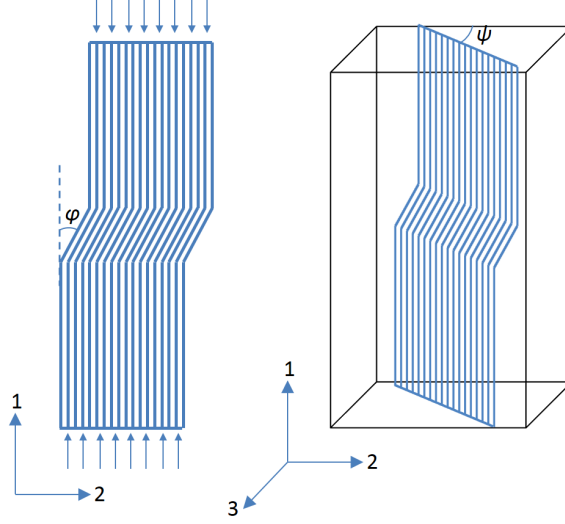
Figure 4.23: Fiber kinking in 2D and 3D

The stress transformation in the kink plane is as follow :

$$\begin{cases} \sigma_{2\psi 2\psi} = \frac{\sigma_{22}+\sigma_{33}}{2} + \frac{\sigma_{22}-\sigma_{33}}{2}cos(2\psi) + \tau_{23}sin(2\psi) \\ \sigma_{3\psi 3\psi} = \sigma_{22} + \sigma_{33} - \sigma_{2\psi 2\psi} \\ \tau_{12\psi} = \tau_{12}cos(\psi) + \tau_{31}sin(\psi) \\ \tau_{2\psi 3\psi} = 0 \\ \tau_{3\psi 1\psi} = \tau_{31}cos(\psi) - \tau_{12}sin(\psi) \end{cases} \qquad (4.20)$$

In the kink plane, the kink angle φ at which angle fiber are misaligned has to be determined to transform the stresses to this angle in the kink plane. The angle φ^c is the misalignment angle for pure compression and defined as :

$$\varphi^c = arctan\left(\frac{1 - \sqrt{1 - 4\left(\frac{S^L}{X^C} + \eta^L\right)\frac{S^L}{X^C}}}{2\left(\frac{S^L}{X^C} + \eta^L\right)} \right) \qquad (4.21)$$

The shear strain $\gamma^c_{1^m 2^m}$ in kink band during pure compression is

$$\gamma^c_{1^m 2^m} = \frac{\varphi^c X^C}{G_{12}} \qquad (4.22)$$

The initial misalignment angle is calculated as :

$$\varphi^0 = \varphi^c - \gamma^c_{1^m 2^m} \qquad (4.23)$$

47

and then shear strain $\gamma_{1^m 2^m}$ for linear shear behaviour is defined as :

$$\gamma_{1^m 2^m} = \frac{\varphi^0 G_{12} + \mid \tau_{12^\psi} \mid}{G_{12} + \sigma_{11} - \sigma_{2^\psi 2^\psi}} - \varphi^0 \tag{4.24}$$

From that, angle φ is obtained

$$\varphi = \frac{\tau_{12^\psi}}{|\tau_{12^\psi}|} \left(\varphi^0 + \gamma_{1^m 2^m} \right) \tag{4.25}$$

Finally, stresses can be transformed into the misalignment angle as

$$\begin{cases} \sigma_{1^m 1^m} = \frac{\sigma_{11} + \sigma_{2^\psi 2^\psi}}{2} + \frac{\sigma_{11} - \sigma_{2^\psi 2^\psi}}{2} cos(2\varphi) + \tau_{12^\psi} sin(2\varphi) \\ \sigma_{2^m 2^m} = \sigma_{11} + \sigma_{2^\psi 2^\psi} - \sigma_{1^m 1^m} \\ \tau_{1^m 2^m} = \frac{\sigma_{11} - \sigma_{2^\psi 2^\psi}}{2} sin(2\varphi) + \tau_{12^\psi} cos(2\varphi) \\ \tau_{2^m 3^\psi} = \tau_{2^\psi 3^\psi} cos(\psi) - \tau_{3^\psi 1} sin(\psi) \\ \tau_{3^\psi 1^m} = \tau_{3^\psi 1^\psi} cos(\psi) \end{cases} \tag{4.26}$$

Then tractions on this plane are calculated as

$$\begin{cases} \sigma_n^m = \frac{\sigma_{2^m 2^m} + \sigma_{3^\psi 3^\psi}}{2} + \frac{\sigma_{2^m 2^m} - \sigma_{3^\psi 3^\psi}}{2} cos(2\alpha) + \tau_{2^m 3^\psi} sin(2\alpha) \\ \tau^{Tm} = -\frac{\sigma_{2^m 2^m} - \sigma_{3^\psi 3^\psi}}{2} sin(2\alpha) + \tau_{2^m 3^\psi} cos(2\alpha) \\ \tau^{Lm} = \tau_{1^m 2^m} cos(\alpha) + \tau_{3^\psi 1^m} sin(\alpha) \end{cases} \tag{4.27}$$

4.7.5 List of failure criteria

Four types of failures are included in LaRC04 criteria. Matrix tensile failure due to matrix cracking is developed on the basis of fracture mechanics and Eshelby's inclusion problem. Matrix compression is based on M-C failure theory. Fiber compression failure is formulated considering fiber kinking and the subsequent effect of matrix tensile failure.Other parameters which needs to define the failure criteria are fracture toughness ratio g and in-plane internal shear strain energy $\chi(\gamma_{12})$ and defined as :

$$g = \frac{G_{Ic}}{G_{IIc}} \tag{4.28}$$

$$\chi(\gamma_{12}) = 2 \int_0^{\gamma_{12}} \tau_{12} d\gamma_{12} \tag{4.29}$$

The failure criteria are given below:

1. Matrix tensile failure $\sigma_{22} \geq 0$

$$FI_M = (1 - g) \frac{\sigma_2}{Y_{is}^T} + g \left(\frac{\sigma_2}{Y_{is}^T} \right)^2 + \frac{\Lambda_{23}^o \tau_{23}^2 + \chi(\gamma_{12})}{\chi\left(\gamma_{12|is}^u\right)} \tag{4.30}$$

2. Matrix compression failure $\sigma_{22} < 0$

$$FI_M = \left(\frac{\tau^{Tm}}{S^T - \eta^T \sigma_n^m} \right)^2 + \left(\frac{\tau^{Lm}}{S_{is}^L - \eta^L \sigma_n^m} \right)^2 , \sigma_{11} < -Y^C \tag{4.31}$$

$$FI_M = \left(\frac{\tau^T}{S^T - \eta^T \sigma_n} \right)^2 + \left(\frac{\tau^L}{S_{is}^L - \eta^L \sigma_n} \right)^2 , \sigma_{11} \geq -Y^C \tag{4.32}$$

3. Fiber tensile failure $\sigma_{11} \geq 0$

$$FI_F = \frac{\sigma_{11}}{X^T} \tag{4.33}$$

4. Fiber compressive failure $\sigma_{11} < 0$

$$FI_F = \frac{|\tau_{1^m 2^m}|}{S_{is}^L - \eta^L \sigma_{2^m 2^m}}, \sigma_{2^m 2^m} < 0 \tag{4.34}$$

$$FI_M = (1-g)\frac{\sigma_{2^m 2^m}}{Y_{is}^T} + g\left(\frac{\sigma_{2^m 2^m}}{Y_{is}^T}\right)^2 + \frac{\Lambda_{23}^o \tau_{2^m 3^\psi}^2 + \chi\left(\gamma_{1^m 2^m}\right)}{\chi\left(\gamma_{12|is}^u\right)}, \sigma_{2^m 2^m} \geq 0 \tag{4.35}$$

4.8   Results and discussions

The load-displacement curve predicted from PDM in case of UD CFRP panel with single hole is shown in Fig. 4.24. PDM with LaRC04 is largely overpredicting the ultimate load and the corresponding displacement. The reason behind this is the matrix compression and fiber compression criteria. The damage state near the hole in the top and bottom ply with increasing load is shown in Fig. 4.25. It can be seen that there is no significant damage in the compression side. Experimentally it is found that damage propagates in transverse direction from the hole but PDM with LaRC04 predicts the damage propagation in the longitudinal direction from the hole. The tension side ply has the damage initiation in the longitudinal direction with matrix tensile failure. With increasing flexural loading, damage also propagates in the transverse direction near the hole in form of fiber tensile failure. It should be noted that there is no damage detected in transverse direction on tension side in the experimental results. Only some longitudinal fiber splitting is found experimentally. The ultimate failure predicted by PDM with LaRC04 is due to the fiber tensile failure. However, experimentally it is found that UD CFRP panel is failed due to matrix and fiber compression failure on the compression side. LaRC04 is overpredicting these two failures.
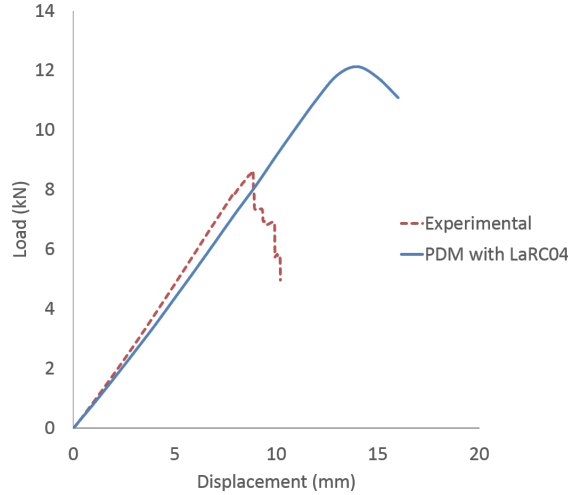

Figure 4.24: Load-displacement predicted by PDM with LaRC04 in case of UD CFRP panel with 1H configuration
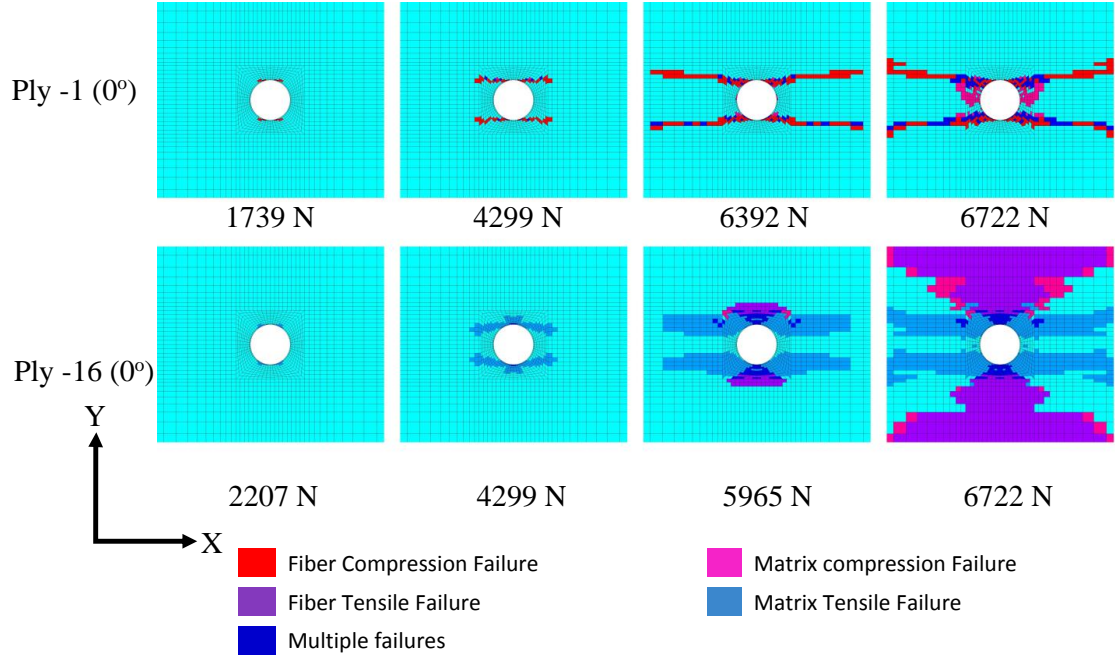
Figure 4.25: Illustration of damage propagation predicted by the PDM (LaRC04) with increasing load for UD CFRP laminate having 1H configuration

Other researchers [44, 45] also have come up with the same outcome. Kottner et al. [44] has suggested the correction in matrix compression and fiber tensile criteria. They included the effect of longitudinal stress in the matrix compression failure criteria. However, those corrections are empirical and solely based on the material they used and experimental observations. They may not fit the failures occurred in the present study. The modified criteria are as follow :

$$FI_M = \left(\frac{\tau^T}{S^T - \eta^T \sigma_n + \sigma_L P_M} \right)^2 + \left(\frac{\tau^L}{S_{is}^L - \eta^L \sigma_n + \sigma_L P_M} \right)^2 , \sigma_{11} \geq -Y^C \qquad (4.36)$$

$$FI_F = \frac{\sigma_L}{X^T P_F}, \sigma_{11} \geq -Y^C \qquad (4.37)$$

where, P_M and P_F are the correction factors and σ_L is the longitudinal stress. The same way, the experimental results in this study can also be fitted with appropriate values of the correction factors. Also the fracture angle can also affect the results. In the absence of experimental data, its value is assumed to be $53°$. This parameter needs to be verified through experiments of simple compression tests. Also it is to be noted that the non-linear shear behaviour is not included in the PDM algorithm with LaRC04. It can be included in PDM with proper experimental characterization of non-linear shear parameters. The damage modelling is done through MPDM rule with degradation upto 5%. The modification in the damage modelling or degradation factor can improve the PDM results. Therefore, there are many approximations included in the PDM algorithm. Some of them needs to be removed to get the accurate PDM predictions.

4.9 Closure

The UD and quasi CFRP panels with different single and multiple holes configurations are analysed using FEA based PDM. Various failure criteria such as Hashin's, Ye's delamination, LaRC04 etc. are used in PDM to predict the failure with employing MPDM rule as damage modelling. Hashin's failure theory predicts the damage well on the tension side. However, the experimental results are not matching with Hashin's or LaRC04 failure criteria mainly due to fiber and matrix compression. Hashin's criteria underpredicts the fiber and compression failure that affects the ultimate failure. The PDM results with Hashin's criteria are summarized in Table 4.3 and 4.4. CFRP panels with 2HL configuration has the highest load carrying capacity among the panels with multiple holes configuration. LaRC04 criteria is overpredicting fiber and matrix compression failures. It is recommended to use LaRC04 over Hashin's failure criteria because it is physics based failure theory. However, it needs to modify the criteria with appropriate corrections and also experimental characterization is required for fracture angle and non-linear shear behaviour. CZM properties are successfully calibrated with experimental results. The delamination through CZM is yet to be implemented in PDM.

Table 4.3: Results of UD CFRP panels with different holes configurations

Configuraion	Experimental		PDM	
	Ultimate Load (kN)	Disp. (mm)	Ultimate Load (kN)	Disp. (mm)
1H	8.595	8.815	6.722	7.0
2HL	8.112	8.333	6.673	7.0
2HD	6.402	7.174	6.674	7.0
2HT	6.165	7.639	5.786	6.5

Table 4.4: Results of quasi CFRP panels with different holes configurations

Configuraion	Experimental		PDM	
	Ultimate Load (kN)	Disp. (mm)	Ultimate Load (kN)	Disp. (mm)
1H	5.152	9.946	3.811	8.5
2HL	5.109	10.441	3.529	7
2HD	4.736	10.348	3.648	8
2HT	4.223	8.507	3.436	8

Chapter 5

Conclusion and recommendation for future work

5.1 Conclusions

The present study is focused on the CFRP panels with multiple hole interacting with each other under flexural loading. Hashin's and LaRC04 failure criteria are used to predict the damage with MPDM for damage modelling.

Flexural longitudinal secant modulus is found out to capture the accurate flexural condition in FEM. It is nearly equal to the longitudinal Young's modulus determined through tensile test. 2D DIC is used to get the full displacement and strain data in all experimental work. Mode-I and mode-II fracture toughness are found out through DCB and ENF tests respectively. A method to determine the mode-I fracture toughness without measuring delamination length is successfully implemented and verified with MBT method. One issue came out is the thickness of the insert length. It is 45 μm instead of 13 μm recommended in ASTM standard. The effect of the thickness on the fracture toughness is still not yet known. The reason behind less difference between mode-I and mode-II fracture toughness has to be found out.

Experimental study is carried out for failure analysis of CFRP panels under flexural loading. In multiple holes, 2HL panel is found out to have high load carrying capacity in both, UD and quasi-isotropic laminate. The compression side is weak and fails first. The damage initiates at the edges of the hole in longitudinal direction and propagates in the transverse direction through holes. The damage in tension side is found out be less compared to compression side. Delamination in quasi-isotropic CFRP panel is found out to be significant than the UD CFRP panels. Final failure occurs in the CFRP panels on the compression side.

3-D based progressive damage modelling is developed for CFRP panel. Hashin's failure criteria underpredicts the ultimate load in all the cases because of the overestimation the fiber and matrix compression failures. Cohesive zone model is calibrated with experimental results and convergence problem is resolved with the help of viscous regularization. Physics based LaRC04 criteria is implemented in the PDM but found out to be overpredicting the final failure load. It observed that failure initiation is captured accurately with these both failure criteria but fail to predict the final failures. However, LaRC04 is recommended over Hashin's due to physical significance given to

different failures in composites in LaRC04.

5.2 Recommendations for future work

It is observed that no present criteria can predict the different failures and ultimate failure accurately. There is lots of scope of improvisation regarding failure criteria. Non-linear shear behaviour can affect the PDM prediction. Therefore, CFRP should be characterise for non-linear behaviour so that it can be included into LaRC04 criteria. One recommendation is to implement continuum damage mechanics model for damage modelling instead of MPDM. The best approach is to develop multiscale model (stress analysis at macro level and damage assessment at microlevel) for composite materials. Also it will be very interesting to study the effect of fiber orientation on the fracture toughness of the CFRP material and can help to model delamination in quasi-isotropic laminates. The fabrication technique should be shifted towards prepregs or vacuum assisted resin infusion moulding (VARIM) to get uniform thickness and lesser void content. Finding delamination length during fracture toughness tests is very difficult task and therefore ther e is need to develop the method to determine the fracture toughness without measuring the delamination length. Bridging the gap between the intralaminar and interlaminar failures is the work that needs a lot of efforts.

References

[1] A. Trilaksono, N. Watanabe, A. Kondo, H. Hoshi, and Y. Iwahori. Automatic Damage Detection and Monitoring of a Stitch Laminate System Using a Fiber Bragg Grating Strain Sensor. *Open Journal of Composite Materials* 2014.

[2] M. Kashfuddoja and M. Ramji. Whole-field strain analysis and damage assessment of adhesively bonded patch repair of CFRP laminates using 3D-DIC and FEA. *Composites Part B: Engineering* 53, (2013) 46–61.

[3] K. T. Kedward. On the short beam test method. *Fibre Science and Technology* 5, (1972) 85–95.

[4] J. Chen, D. Tu, and H. Chin. Elastic-plastic analysis of interlaminar stresses in composite laminates due to bending and torsion. *Computers & structures* 33, (1989) 385–393.

[5] M. Wisnom. The effect of specimen size on the bending strength of unidirectional carbon fibre-epoxy. *Composite Structures* 18, (1991) 47–63.

[6] Y. Reddy and J. Reddy. Linear and non-linear failure analysis of composite laminates with transverse shear. *Composites Science and Technology* 44, (1992) 227–255.

[7] W. Cui and M. Wisnom. A combined stress-based and fracture-mechanics-based model for predicting delamination in composites. *Composites* 24, (1993) 467–474.

[8] J. Echaabi, F. Trochu, X. Pham, and M. Ouellet. Theoretical and experimental investigation of failure and damage progression of graphite-epoxy composites in flexural bending test. *Journal of reinforced plastics and composites* 15, (1996) 740–755.

[9] E. H. Irhirane, J. Echaabi, M. Aboussaleh, M. Hattabi, and F. Trochu. Matrix and Fibre Stiffness Degradation of a Quasi-isotrope Graphite Epoxy Laminate Under Flexural Bending Test. *Journal of Reinforced Plastics and Composites* .

[10] G. Padhi, R. Shenoi, S. Moy, and G. Hawkins. Progressive failure and ultimate collapse of laminated composite plates in bending. *Composite structures* 40, (1997) 277–291.

[11] L. Dufort, M. Grédiac, and Y. Surrel. Experimental evidence of the cross-section warping in short composite beams under three point bending. *Composite Structures* 51, (2001) 37–47.

[12] P. Feraboli and K. Kedward. Four-point bend interlaminar shear testing of uni-and multi-directional carbon/epoxy composite systems. *Composites Part A: Applied Science and Manufacturing* 34, (2003) 1265–1271.

[13] F. Bosia, M. Facchini, J. Botsis, T. Gmür, and D. de'Sena. Through-the-thickness distribution of strains in laminated composite plates subjected to bending. *Composites science and technology* 64, (2004) 71–82.

[14] A. Turon, P. P. Camanho, J. Costa, and C. Dávila. A damage model for the simulation of delamination in advanced composites under variable-mode loading. *Mechanics of Materials* 38, (2006) 1072–1089.

[15] M. Mulle, R. Zitoune, F. Collombet, L. Robert, and Y.-H. Grunevald. Embedded FBGs and 3-D DIC for the stress analysis of a structural specimen subjected to bending. *Composite Structures* 91, (2009) 48–55.

[16] C. Santiuste, S. Sánchez-Sáez, and E. Barbero. A comparison of progressive-failure criteria in the prediction of the dynamic bending failure of composite laminated beams. *Composite Structures* 92, (2010) 2406–2414.

[17] G. Ernst, M. Vogler, C. Hühne, and R. Rolfes. Multiscale progressive failure analysis of textile composites. *Composites Science and Technology* 70, (2010) 61–72.

[18] H. Ullah, A. R. Harland, T. Lucas, D. Price, and V. V. Silberschmidt. Finite-element modelling of bending of CFRP laminates: Multiple delaminations. *Computational Materials Science* 52, (2012) 147–156.

[19] A. Makeev, Y. He, B. Shonkwiler, E. Lee, H. Schreier, and Y. Nikishkov. A method for measurement of three-dimensional constitutive properties for composite materials. In Proceedings of the 18th international conference on composite materials (ICCM18). South Korea. 2011 21–26.

[20] Y. He, A. Makeev, and B. Shonkwiler. Characterization of nonlinear shear properties for composite materials using digital image correlation and finite element analysis. *Composites Science and Technology* 73, (2012) 64–71.

[21] A. Puck and S. W. On failure mechanisms and failure criteria of filament-wound glass-fibre/resin composites. *Plastics & Polymers* 37, (1969) 33.

[22] Z. Hashin. Failure criteria for unidirectional fiber composites. *Journal of applied mechanics* 47, (1980) 329–334.

[23] S. W. Tsai and E. M. Wu. A general theory of strength for anisotropic materials. *Journal of composite materials* 5, (1971) 58–80.

[24] L. Hart-Smith. Predictions of a generalized maximum-shear-stress failure criterion for certain fibrous composite laminates. *Composites Science and Technology* 58, (1998) 1179–1208.

[25] C. Sun and J. Tao. Prediction of failure envelopes and stress/strain behaviour of composite laminates. *Composites Science and technology* 58, (1998) 1125–1136.

[26] L. McCartney. Predicting transverse crack formation in cross-ply laminates. *Composites Science and Technology* 58, (1998) 1069–1081.

[27] M. J. Hinton, A. S. Kaddour, and P. D. Soden. Failure criteria in fibre reinforced polymer composites: the world-wide failure exercise. Elsevier, 2004.

[28] S. T. Pinho, C. G. Dàvila, P. P. Camanho, L. Iannucci, and P. Robinson. Failure models and criteria for FRP under in-plane or three-dimensional stress states including shear non-linearity. *NASA Technical Memorandum* 213530, (2005) 18.

[29] D. Dugdale. Yielding of steel sheets containing slits. *Journal of the Mechanics and Physics of Solids* 8, (1960) 100–104.

[30] G. I. Barenblatt. The mathematical theory of equilibrium cracks in brittle fracture. *Advances in applied mechanics* 7, (1962) 55–129.

[31] A. Hillerborg, M. Modéer, and P.-E. Petersson. Analysis of crack formation and crack growth in concrete by means of fracture mechanics and finite elements. *Cement and concrete research* 6, (1976) 773–781.

[32] V. Tvergaard and J. W. Hutchinson. The relation between crack growth resistance and fracture process parameters in elastic-plastic solids. *Journal of the Mechanics and Physics of Solids* 40, (1992) 1377–1397.

[33] X.-P. Xu and A. Needleman. Numerical simulations of fast crack growth in brittle solids. *Journal of the Mechanics and Physics of Solids* 42, (1994) 1397–1434.

[34] A. Turon, C. G. Davila, P. P. Camanho, and J. Costa. An engineering solution for mesh size effects in the simulation of delamination using cohesive zone models. *Engineering fracture mechanics* 74, (2007) 1665–1682.

[35] A. Standard. D7264M-15. *Standard Test Method for Flexural Properties of Polymer Matrix Composite Materials, ASTM International, West Conshohocken, PA* .

[36] A. Standard. D5528-01. *Standard Test Method for Mode I Interlaminar Fracture Toughness of Unidirectional Fiber-Reinforced Polymer Matrix Composites, ASTM International, West Conshohocken, PA* .

[37] D. Svensson. Experimental methods to determine model parameters for failure modes of CFRP. Ph.D. thesis, Ph. D. thesis. Chalmers University Gothenburg 2013.

[38] A. Biel and U. Stigh. An analysis of the evaluation of the fracture energy using the DCB-specimen. *Archives of Mechanics* 59, (2007) 311–327.

[39] A. Standard. D7905M-14. *Standard Test Method for Determination of the Mode II Interlaminar Fracture Toughness of Unidirectional Fiber-Reinforced Polymer Matrix Composites, ASTM International, West Conshohocken, PA* .

[40] ANSYS, Inc. ANSYS Mechanical APDL Contact Technology Guide 2013.

[41] M. Kashfuddoja and M. Ramji. An experimental and numerical investigation of progressive damage analysis in bonded patch repaired CFRP laminates. *Journal of Composite Materials* 49, (2015) 439–456.

[42] M. Kashfuddoja, R. Prasath, and M. Ramji. Study on experimental characterization of carbon fiber reinforced polymer panel using digital image correlation: A sensitivity analysis. *Optics and Lasers in Engineering* 62, (2014) 17–30.

[43] Y. Gao and A. Bower. A simple technique for avoiding convergence problems in finite element simulations of crack nucleation and growth on cohesive interfaces. *Modelling and Simulation in Materials Science and Engineering* 12, (2004) 453.

[44] R. Kottner, T. Kroupa, V. Laš, and K. Blahouš. Computational Model for Strength Analysis of Wrapped Pin Joint of Composite/Metal. *Bulletin of Applied Mechanics* 4, (2008) 1–6.

[45] E. Totry, C. González, and J. LLorca. Prediction of the failure locus of C/PEEK composites under transverse compression and longitudinal shear through computational micromechanics. *Composites Science and Technology* 68, (2008) 3128–3136.